Faculty of Natural and Applied Sciences Journal of Scientific Innovations
Print ISSN: 2814-0877 e-ISSN: 2814-0923
www.fnasjournals.com
Volume 6; Issue 1; September 2024; Page No. 84-108.

A Fractional-Order Model for Zika Virus Transmission Dynamics: Analysis, Control Strategies, and Simulation Insights

Loyinmi, A. C.
Tai Solarin University of Education, Ijagun. Ogun State. Nigeria

Corresponding author e-mail: loyinmiac@tasued.edu.ng

Abstract
The Zika virus, characterized by its complex transmission dynamics, poses a significant public health challenge. This study presents a novel mathematical model employing Caputo fractional derivatives to capture the intricate dynamics of the transmission of Zika virus between human and vector populations. Whereas the vector population is split into susceptible, exposed, and infected groups, the human population is classified into susceptible, exposed, asymptomatic, symptomatic, and recovered people. Our model incorporates fractional-order dynamics to better account for memory effects and historical data, which are often overlooked in classical models. Positivity and boundedness analyses verify the validity of the model, guaranteeing that all state variables are bounded and non-negative throughout time. Furthermore, the Banach contraction mapping theorem is used to prove the solution's existence and uniqueness. The next-generation matrix approach is used to obtain the fundamental reproduction number (R_0), which sheds light on the prerequisites for both disease persistence and outbreak. Numerical simulations illustrate the model's dynamics, revealing the impact of fractional orders on disease spread. Optimal control strategies, including vaccination, treatment, and environmental management, are integrated into the model to assess their effectiveness in mitigating the virus's transmission. The simulations demonstrate that optimal control measures significantly lower the number of infected individuals in both human as well as vector populations, although the complexities of vector management highlight the need for careful calibration of interventions. Our findings underscore the enhanced descriptive power of fractional-order models in capturing the real-world complexities of Zika virus transmission. This model offers a robust framework for public health officials to design and implement more effective control strategies, ultimately contributing to better management of Zika virus outbreaks and other vector-borne diseases.

Keywords: Zika Virus, Fractional Differential Equations, Epidemiological Modeling; Caputo Derivative; Optimal Control Strategies

Introduction

The Zika virus, a member of the Flaviviridae family mostly spread by Aedes mosquitoes, has become a major worldwide health issue because of its link to serious neurological problems and adverse pregnancy outcomes. This introduction aims to give a comprehensive overview of Zika virus, including information on its epidemiology, clinical signs and symptoms, complications, prevention strategies, and the World Health Organization's (WHO) and other stakeholders' continuing response activities. The Zika virus was first discovered in the Ugandan Zika forest in 1947, but it was not well known until outbreaks in Micronesia in 2007 and French Polynesia in 2013–2014 brought it to the attention of the world. But it was the 2015 Zika outbreak in Brazil that caused the most alarm, especially since it was linked to a rise in cases of microcephaly in children whose mothers had contracted the virus while they were pregnant. Aedes mosquitoes are the principal vectors of the Zika virus, with Aedes aegypti serving as the primary vector for human transmission (De Araujo et al., 2022: Muso & Baud., 2019). Since these mosquitoes are usually active throughout the day, there is a higher chance of becoming exposed. Furthermore, during pregnancy, the Zika virus can also spread vertically from mother to foetus through intercourse, transfusions of blood, and potentially organ transplants (Griffin, 2012). The ability of Zika virus to be transmitted through multiple routes underscores the complexity of its control and prevention. Most individuals infected with Zika virus are asymptomatic, and those who develop symptoms typically experience mild and self-limiting illness, including rash,

fever, conjunctivitis, muscle and joint pain, malaise, and headache (Agusto et al., 2017; Andraud et al., 2012). The greatest worry, though, is that a pregnant woman may contract the Zika virus, which could result in serious prenatal defects like microcephaly and other neurological complications like adult Guillain-Barré syndrome. The World Health Organization (WHO) announced a Public Health Emergency of International Concern (PHEIC) in February 2016 in response to the Zika virus's growing threat. This declaration underscored the urgent need for concerted global effort to address the propagation of Zika virus and its associated complications (Gonzlez-Parra et al., 2020). While the PHEIC was lifted in November of the same year, the ongoing transmission of Zika virus in various regions, particularly in the Americas, underscores the continued importance of vigilance and response efforts.

Efforts to combat Zika virus are multifaceted and encompass both prevention and control strategies. Key among these is vector control, which aims to lower the amount of mosquitoes and reduce human-mosquito interaction. This involves measures including removing mosquito breeding grounds, applying insecticides, and putting in place neighbourhood-based mosquito control programs. Insect repellents, long sleeves and sleeping under mosquito nets are examples of private safety measures that are crucial in preventing mosquito bites and reducing the risk of Zika virus transmission (Hayes, 2009; Grifin, 2012). In light of the possibility of sexual transmission of the Zika virus, especially between expectant mothers and their partners, sexual health education and counselling are essential components of prevention efforts. Recommendations include practising safer sex or abstinence, especially for those who reside in or return from places where the Zika virus is currently transmitted. Pregnant women are advised to seek medical attention for testing and counselling, while those planning pregnancy are encouraged to consider the risks associated with the Zika virus and take appropriate precautions (Idowu & Loyinmi., 2023; Khan et al., 2019). In addition to prevention, efforts to improve diagnostic capabilities and clinical management are essential for addressing Zika virus infections effectively. Laboratory confirmation of Zika virus infection is necessary due to the overlap in symptoms with other arboviral diseases, such as dengue and chikungunya. However, access to reliable diagnostic tests remains limited in many regions, highlighting the need for increased investment in diagnostic infrastructure and capacity building (Loyinmi et al., 2024; Loyinmi et al., 2021). Despite advances in understanding the Zika virus, no vaccine or targeted antiviral therapy is presently available to treat Zika virus infection. Research efforts are ongoing to develop vaccines and therapeutics, but significant challenges remain, including the complex nature of the virus and the limited understanding of its pathogenesis.

The World Health Organization (WHO) has been at the forefront of organizing international efforts to prevent, detect, and contain epidemics in response to the Zika virus threat. This includes supporting countries in surveillance, laboratory testing, vector control, and clinical management. WHO has also issued guidelines and recommendations for the prevention and control of the Zika virus, aimed at guiding national and international response efforts. The Zika virus poses a complicated and dynamic public health threat that has consequences for the security of global health and while progress has been made in understanding the virus and implementing control measures, continued vigilance and investment are essential to prevent future outbreaks and mitigate the impact of Zika virus on vulnerable populations. By addressing the multifaceted aspects of Zika virus transmission, clinical management, and prevention, stakeholders may collaborate to mitigate the impact of this emerging infectious disease and safeguard the health and welfare of people across the globe.

Efforts to develop a Zika virus vaccine have led to several promising approaches. One pioneering effort by the National Institute of Allergy and Infectious Diseases' (NIAID) Vaccine Research Center (VRC) involves a DNA-based vaccine. This vaccine, similar to one developed for West Nile virus, uses a DNA segment to induce an immune response. Initial Phase 1 trials began in August 2016, with an optimized version tested later that year. These trials showed that the vaccine induced a neutralizing antibody response and was safe. A Phase 2 trial, VRC 705, started in March 2017 to further assess safety, immunogenicity, and efficacy in preventing Zika infection (Yun & Lee., 2017). Another promising approach is the purified inactivated Zika vaccine (ZPIV) developed by the Walter Reed Army Institute of Research (WRAIR), which builds on strategies used for Japanese Encephalitis and dengue vaccines (Loyinmi & Gbodogbe, 2024; Sikka et al., 2016). Phase 1 trials at multiple sites confirmed its safety and immunogenicity. NIAID's Laboratory of Viral Diseases developed an investigational live attenuated vaccine, rZIKV/D4Δ30-713, combining dengue and Zika virus genetic material. This candidate entered Phase 1 trials in August 2018 and could potentially be combined with a dengue vaccine. Additionally, mRNA vaccines, being evaluated in collaboration with GlaxoSmithKline and Moderna, offer rapid development and scalability. The investigational AGS-v vaccine targets mosquito saliva proteins to prevent multiple mosquito-borne diseases. Lastly,

Cite this article as:
Loyinmi, A. C. (2024). A fractional-order model for zika virus transmission dynamics: analysis, control strategies, and simulation insights, *FNAS Journal of Scientific Innovations, 6*(1), 84-108.

a vaccine using vesicular stomatitis virus (VSV), successful in Ebola vaccines, is in the early development stages for Zika.

Controlling the spread of Zika Virus (ZIKV) primarily hinges on managing the Aedes mosquito population, as these mosquitoes are the primary vectors for transmission (Tesla et al., 2018; Padmanabhan et al., 2017). High-density human populations, lack of immunity, virus mutations, and global warming all contribute to the propagation of ZIKV. Despite various transmission modes, prioritizing mosquito control is crucial. Effective measures include mechanical, biological, and chemical strategies to prevent mosquito breeding and reduce their population. Chemical control, while effective, poses risks such as resistance and bioaccumulation, prompting a shift toward biopesticides (Duffy et al., 2009; Bearcroft, 1956). Plant extracts and essential oils have shown promise in mosquito control. Additionally, bacteria like Wolbachia pipientis can disrupt mosquito reproduction and reduce virus transmission. Genetic engineering techniques, such as using siRNA to induce male sterility, offer another avenue for control. Fungi and fish are also explored for their potential to control mosquito populations, though further research is needed to ensure their viability and ecological safety. Given the absence of a commercial ZIKV vaccine, significant advancements are being made in vaccine development. Several candidates are in the preclinical and clinical phases, with transmission-blocking vaccines (TBVs) showing great promise (Loyinmi & Gbodogbe., 2024). These vaccines prevent the spread of the virus from infected to naive individuals, potentially benefiting entire communities. Utilizing fields like immune profiling, bioinformatics, and reverse immunology could accelerate the development of effective and cost-efficient ZIKV vaccines (Idowu & Loyinmi., 2023; Khan & Atangana., 2020; Agbomola & Loyinmi., 2022). Public education on mosquito-repelling herbal products, which are safe for all individuals including pregnant women, is vital. Protecting health workers and ensuring safe blood and organ donations are also critical (Krauer et al., 2017; Mehrjardi, 2017). Globalization and climate change have exacerbated the spread of ZIKV, necessitating infrastructure improvements and effective public health strategies. Understanding all transmission modes, educating pregnant women on travel risks, and enhancing epidemiological data are essential for comprehensive control efforts. International cooperation and data sharing on mosquito control are crucial for global ZIKV management, alongside rapid vaccine development to bring effective solutions to market.

Researchers across various scientific and engineering disciplines have recently shown a growing interest in utilizing fractional differential equations for mathematical modelling, particularly in epidemiology (Loyinmi & Ijaola., 2024; Khan & Atangana., 2020; Rezapour et al., 2020). Fractional-order models offer unique advantages over classical differential equations, mainly due to their ability to incorporate memory effects, a characteristic absent in classical models. This property stems from the inherent features of fractional differential equations, which account for the historical behaviour of a system, providing a more comprehensive understanding of dynamic processes. Fractional differential equations have been increasingly employed to model both infectious and non-infectious diseases (Loyinmi et al., 2024; Banuelos et al., 2019). One prominent example is the extensive research on Zika virus, where fractional models have yielded significant insights. Studies using fractional-order models based on the Caputo derivative have effectively captured the complex dynamics of Zika virus transmission and control measures. Similarly, tuberculosis has been studied using fractional-order models that consider endogenous reactivation and exogenous reinfections, providing a nuanced understanding of disease progression and recurrence. In the context of HIV/AIDS, researchers have developed fractional-order epidemic models incorporating the Mittag-Leffler kernel. This approach has facilitated the analysis of the disease's spread and the impact of various intervention strategies. The flexibility and adaptability of fractional-order models have also been demonstrated in studies of other diseases, showcasing their broad applicability and effectiveness. Contrastingly, classical differential equations, which rely on integer-order derivatives, lack the ability to capture the memory and hereditary properties of complex systems. While classical models have been instrumental in advancing epidemiological studies, they often fall short of accurately representing the long-term dependencies and non-local behaviours observed in real-world scenarios (Alfwan et al., 2023; Kibona & Yang., 2017). Fractional-order models bridge this gap by offering a more detailed and accurate depiction of disease dynamics, accounting for past states and interactions over time. The increasing application of fractional differential equations in epidemiology highlights their potential to enhance our understanding of disease mechanisms and improve the effectiveness of control and prevention strategies. By integrating memory effects and historical data, fractional-order models provide a powerful tool for researchers and public health officials to address current and future challenges in disease modelling and management.

Our central aim is to delve into the intricate dynamics, efficacy of control strategies, and computational estimations inherent in the fractional-order Zika virus model under scrutiny. Our inquiry begins by scrutinizing the model's

Cite this article as:
Loyinmi, A. C. (2024). A fractional-order model for zika virus transmission dynamics: analysis, control strategies, and simulation insights, *FNAS Journal of Scientific Innovations*, *6*(1), 84-108.

positivity and constraining attributes through conventional mathematical analysis techniques. Following this, we ascertain the fundamental reproduction number utilizing the next-generation matrix approach and assess the model's asymptotic stability. Furthermore, employing an adaptive predictor-corrector algorithm alongside the fourth-order Runge–Kutta (RK4) method, we conduct comprehensive numerical simulations, thereby validating the theoretical insights across a broad spectrum of scenarios. This multifaceted approach ensures a robust examination of the model's behaviour and underpins our understanding through rigorous computational analysis.

The theory of fractional calculus

In this section, we shall acquaint ourselves with the fundamental concepts and nomenclature of fractional calculus theory, primed for its application in scrutinizing the infectious disease model at hand. Furthermore, its multifarious utility spans a spectrum of scientific domains.

Definition 1. The fractional integral of Riemann-Liouville order α with respect to a function f, denoted as $f:\Re^{+}\to\Re$, is defined as:

$$I^{\alpha}f(t)=\frac{1}{\Gamma(\alpha)}\int_{0}^{t}(t-\eta)^{\alpha-1}f(\eta)d\eta, \tag{1}$$

Definition 2. The Caputo derivative of a function $g(t)$ over the interval [0, T] can be denoted as:

$${}_{a}^{b}D_{t}^{\alpha}g(t)=\frac{1}{\Gamma(k-\alpha)}\int_{a}^{t}(t-\eta)^{k-\alpha-1}g^{(k)}(\eta)d\eta, \tag{2}$$

Where $k=|\eta|+1$ and $|\eta|$ represents the integer part of η in $[0,1]$.

Definition 3. The Laplace transform of the Caputo derivative can be represented as:

$$L\left\{{}_{a}^{b}D_{t}^{\alpha}g(t)\right\}=S^{\alpha}G(s)-\sum_{n=0}^{m-1}g^{n}(0)S^{\alpha-n-1} \tag{3}$$

Definition 4. The Mittage-Liffler function $E_{\alpha,\alpha+\beta}(\mathrm{Y})$ can be expressed as

$$E_{\alpha,\alpha+\beta}(\mathrm{Y})=\frac{1}{\Gamma(\beta)}+\mathrm{Y}.E_{\alpha,\alpha+\beta}(\mathrm{Y}) \tag{4}$$

Definition 5. The Laplace transform of the function $t^{\beta-1}E_{\alpha,\beta}(\pm\mu t^{\alpha})$ can be written has

$$L\left\{t^{\beta-1}E_{\alpha,\beta}(\pm\mu t^{\alpha})\right\}=\frac{S^{\alpha-\beta}}{S^{\alpha}\mp\mu} \tag{5}$$

Where the two-parameter Mittage–Leffler function is $E_{\alpha,\beta}(t)$, with $\alpha,\beta>0$.

General Mean Value Theorem: Let $g(t)\in b[a,c]$ and ${}_{a}^{b}D_{\beta}^{\zeta}g(\beta)\in b[a,c]$ for $0<\alpha\le 1.$

Then $g(t)$ is:

$$g(t)=g(a)+\frac{1}{\Gamma(\alpha+1)}{}_{a}^{b}D_{\beta}^{\alpha}g(\beta).(t-a)^{\alpha} \text{ where } a\le\beta\le\alpha,\ \forall\alpha\in(a,c]. \tag{6}$$

Also, if ${}_{a}^{b}D_{\alpha_0}^{\alpha}g(\alpha_0)>0,\alpha_0\in(a,c)$, then $\exists$ neighborhood N of α_0, such that

Cite this article as:
Loyinmi, A. C. (2024). A fractional-order model for zika virus transmission dynamics: analysis, control strategies, and simulation insights, *FNAS Journal of Scientific Innovations*, *6*(1), 84-108.

$g(t) > g(a), \forall t \in N$. Otherwise if ${}_a^b D_{\alpha_0}^{\zeta} g(\alpha_0) < 0, \alpha_0 \in (a,c)$, then $\exists$ neighborhood N of α_0, such that $g(t) < g(a), \forall t \in N$.

Model description and formulation

The Zika virus exhibits distinctive transmission dynamics, characterized by a comprehensive population structure that is segmented into two separate cohorts: one dedicated to humans (Np), another to vectors population (Nv). The human population is further divided based on individuals' infection status, including those vulnerable to the Zika Virus (Sp), exposed individuals (Ep), exposed individuals that are not showing clinical symptoms (Iap), exposed individuals with clinical symptoms (Isp), symptomatic individuals undergoing treatment and those who have successfully recovered (Rp) from the infection. The vector population is similarly classified into three categories: vector susceptible to the zika virus (Sp) who have not been infected yet, exposed vector (Ev), and infected vector (Iv) carrying the Zika virus. The flow chart of this model is illustrated in **Error! Reference source not found.**:

The force of infection for both human and vector populations are given as follows:

$$\omega_p{}^{\alpha} = (\theta_1 I_{sp} + \theta_2 I_{AP} + \theta_3 I_v) S_p$$

$$\omega_v{}^{\alpha} = (\theta_4 I_{sp} + \theta_5 I_{AP}) S_v$$

Table 1 provides detailed descriptions of the parameters governing transitions between these compartments within the model, elucidating the Zika Virus transmission dynamics as well as the impact of interventions.

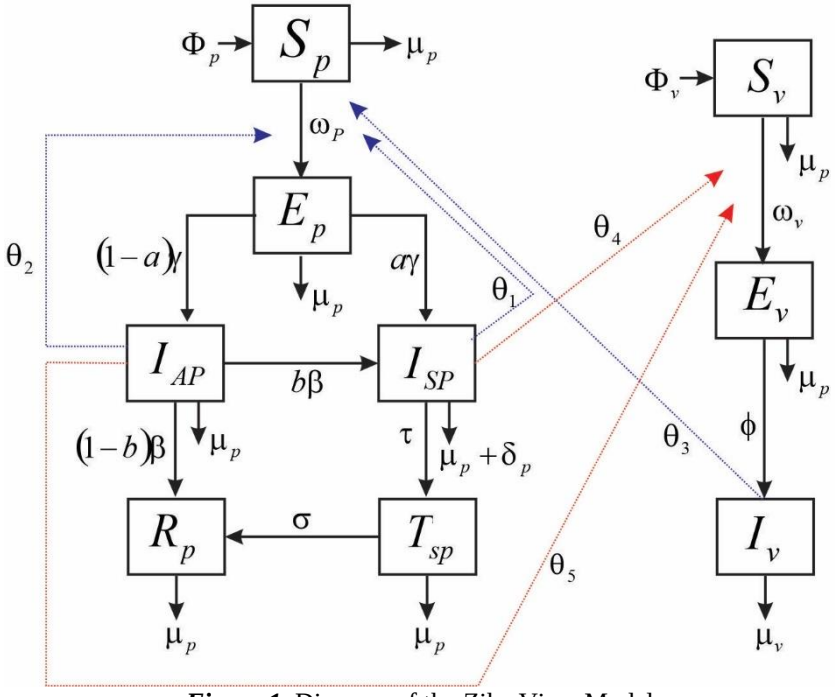

Figure 1. Diagram of the Zika Virus Model

The equation governing the Zika virus model of Caputo fractional derivatives can be expressed as follows:

Cite this article as:
Loyinmi, A. C. (2024). A fractional-order model for zika virus transmission dynamics: analysis, control strategies, and simulation insights, *FNAS Journal of Scientific Innovations*, *6*(1), 84-108.

$$
\left.
\begin{aligned}
{}_0^c D_t^\alpha S_p &= \Phi_p{}^\alpha - \left(\omega_p{}^\alpha + \mu_p{}^\alpha\right) S_p \\
{}_0^c D_t^\alpha E_p &= \omega_p{}^\alpha S_p - \left(\left(1-a^\alpha\right)\gamma^\alpha + a^\alpha\gamma^\alpha + \mu_p{}^\alpha\right) E_p \\
{}_0^c D_t^\alpha I_{AP} &= \left(1-a\right)\gamma^\alpha E_p - \left(\left(1-b^\alpha\right)\beta^\alpha + b^\alpha\beta^\alpha + \mu_p{}^\alpha\right) I_{AP} \\
{}_0^c D_t^\alpha I_{SP} &= a^\alpha\gamma^\alpha E_p + b^\alpha\beta^\alpha I_{AP} - \left(\tau^\alpha + \mu_p{}^\alpha + \delta_p{}^\alpha\right) I_{SP} \\
{}_0^c D_t^\alpha T_{SP} &= \tau^\alpha I_{SP} - \left(\sigma^\alpha + \mu_p{}^\alpha\right) T_{SP} \\
{}_0^c D_t^\alpha R_P &= \left(1-b^\alpha\right)\beta^\alpha I_{AP} + \sigma^\alpha T_{SP} - \mu_p{}^\alpha R_P \\
{}_0^c D_t^\alpha S_v &= \Phi_v{}^\alpha - \left(\omega_v{}^\alpha + \mu_v{}^\alpha\right) S_V \\
{}_0^c D_t^\alpha E_v &= \omega_v{}^\alpha S_v - \left(\phi^\alpha + \mu_v{}^\alpha\right) E_v \\
{}_0^c D_t^\alpha I_v &= \phi^\alpha E_v - \mu_v{}^\alpha I_v
\end{aligned}
\right\} \tag{7}
$$

Where, $\omega_p{}^\alpha = \left(\theta_1 I_{sp} + \theta_2 I_{AP} + \theta_3 I_v\right) S_p$ and $\omega_v{}^\alpha = \left(\theta_4 I_{sp} + \theta_5 I_{AP}\right) S_v$,

And the initial condition is given has

$$S_p(0) \geq 0, E_p(0) \geq 0, I_{Ap}(0) \geq 0, I_{SP}(0) \geq 0, T_{SP}(0) \geq 0, R_P(0) \geq 0, S_v(0) \geq 0, E_V(0) \geq 0, I_v(0)$$

Table 1. **Variables of the Model**

Variables	Description	Values	References
Φ_p	Birth rate in the human susceptible class	300	Estimate
μ_p	Mortality rate of human population	0.00019204	Padmanabhan et al, 2017
a	Proportion of exposed humans who are symptomatic	0.18	Duffy et al, 2009
b	Proportion of asymptomatic humans who are symptomatic	0.5	Estimated
γ	Latency period of the virus in humans	0.2	Bearcroft 1956
β	Transition rate of asymptomatic to symptomatic	0.2	Padmanabhan et al, 2017
τ	The transition rate of symptomatic humans to treated compartments	0.9	Assumed
δ_p	Zika virus-induced rate	0.00071429	Assumed
σ	Recovered rate of treated individual	0.05	Estimated
Φ_v	Recruitment rate of vectors	0.04	Banuelos et al, 2019
μ_v	Vector's lifespan	0.04	Griffin 2012
ϕ	Latency period of Zika virus in vectors	0.1	Andraud et al, 2012
θ_1	Symptomatic human-to-susceptible human contact rate	0.1	Banuelos et al, 2019
θ_2	Asymptomatic human to susceptible human contact rate	0.0992	Banuelos et al, 2019
θ_3	Vector to human contact rate	0.4	Banuelos et al, 2019
θ_4	Symptomatic human-to-vector contact rate	0.5	Banuelos et al, 2019
θ_5	Asymptomatic human-to-vector contact rate	0.5	Banuelos et al. 2019

Cite this article as:
Loyinmi, A. C. (2024). A fractional-order model for zika virus transmission dynamics: analysis, control strategies, and simulation insights, *FNAS Journal of Scientific Innovations*, *6*(1), 84-108.

Analysis of the fractional model

Positivity of Solution

Given that the fractional model (7) observes the human and vector population, it is imperative to demonstrate that all state variables remain positive throughout $t > 0$.

Theorem 1

Consider the initial

$$\left\{S_p(0) \geq 0, E_p(0) \geq 0, I_{Ap}(0) \geq 0, I_{SP}(0) \geq 0, T_{SP}(0) \geq 0, R_P(0) \geq 0, S_v(0) \geq 0, E_V(0) \geq 0, I_v(0)\right\} \varepsilon D.$$

The solution domain $\{S_p, E_p, I_{Ap}, I_{SP}, T_{SP}, R_P, S_v, E_V, I_v\}$ of the fractional model exhibits positivity across all parameters within the invariant region $D \subset \Re_+^9$.

Proof

Recall equations 7

$$\left.\begin{aligned}
{}_0^cD_t^\alpha S_p &= \Phi_p{}^\alpha - \left(\omega_p{}^\alpha + \mu_p{}^\alpha\right)S_p \\
{}_0^cD_t^\alpha E_p &= \omega_p{}^\alpha S_p - \left(\left(1-a^\alpha\right)\gamma^\alpha + a^\alpha\gamma^\alpha + \mu_p{}^\alpha\right)E_p \\
{}_0^cD_t^\alpha I_{AP} &= (1-a)\gamma^\alpha E_p - \left(\left(1-b^\alpha\right)\beta^\alpha + b^\alpha\beta^\alpha + \mu_p{}^\alpha\right)I_{AP} \\
{}_0^cD_t^\alpha I_{SP} &= a^\alpha\gamma^\alpha E_p + b^\alpha\beta^\alpha I_{AP} - \left(\tau^\alpha + \mu_p{}^\alpha + \delta_p{}^\alpha\right)I_{SP} \\
{}_0^cD_t^\alpha T_{SP} &= \tau^\alpha I_{SP} - \left(\sigma^\alpha + \mu_p{}^\alpha\right)T_{SP} \\
{}_0^cD_t^\alpha R_P &= \left(1-b^\alpha\right)\beta^\alpha I_{AP} + \sigma^\alpha T_{SP} - \mu_p{}^\alpha R_P \\
{}_0^cD_t^\alpha S_v &= \Phi_v{}^\alpha - \left(\omega_v{}^\alpha + \mu_v{}^\alpha\right)S_v \\
{}_0^cD_t^\alpha E_v &= \omega_v{}^\alpha S_v - \left(\phi^\alpha + \mu_v{}^\alpha\right)E_v \\
{}_0^cD_t^\alpha I_v &= \phi^\alpha E_v - \mu_v{}^\alpha I_v
\end{aligned}\right\}$$

The solution of the model (7) along one state axis, where other state variables vanish, gives

$$\left.\begin{aligned}
{}_0^cD_t^\alpha S_p\,|_{S_p-axis} &= \Phi_p{}^\alpha - \left(\omega_p{}^\alpha + \mu_p{}^\alpha\right)S_p \\
{}_0^cD_t^\alpha E_p\,|_{E_p-axis} &= \omega_p{}^\alpha S_p - \left(\left(1-a^\alpha\right)\gamma^\alpha + a^\alpha\gamma^\alpha + \mu_p{}^\alpha\right)E_p \\
{}_0^cD_t^\alpha I_{AP}\,|_{I_{AP}-axis} &= (1-a)\gamma^\alpha E_p - \left(\left(1-b^\alpha\right)\beta^\alpha + b^\alpha\beta^\alpha + \mu_p{}^\alpha\right)I_{AP} \\
{}_0^cD_t^\alpha I_{SP}\,|_{I_{SP}-axis} &= a^\alpha\gamma^\alpha E_p + b^\alpha\beta^\alpha I_{AP} - \left(\tau^\alpha + \mu_p{}^\alpha + \delta_p{}^\alpha\right)I_{SP} \\
{}_0^cD_t^\alpha T_{SP}\,|_{T_{SP}-axis} &= \tau^\alpha I_{SP} - \left(\sigma^\alpha + \mu_p{}^\alpha\right)T_{SP} \\
{}_0^cD_t^\alpha R_P\,|_{R_P-axis} &= \left(1-b^\alpha\right)\beta^\alpha I_{AP} + \sigma^\alpha T_{SP} - \mu_p{}^\alpha R_P \\
{}_0^cD_t^\alpha S_v\,|_{S_v-axis} &= \Phi_v{}^\alpha - \left(\omega_v{}^\alpha + \mu_v{}^\alpha\right)S_v \\
{}_0^cD_t^\alpha E_v\,|_{E_v-axis} &= \omega_v{}^\alpha S_v - \left(\phi^\alpha + \mu_v{}^\alpha\right)E_v \\
{}_0^cD_t^\alpha I_v\,|_{I_v-axis} &= \phi^\alpha E_v - \mu_v{}^\alpha I_v
\end{aligned}\right\} \quad (8)$$

Following the same procedures done for the boundedness of the solution, the solution for the above equations is given as,

(9)

Cite this article as:
Loyinmi, A. C. (2024). A fractional-order model for zika virus transmission dynamics: analysis, control strategies, and simulation insights, *FNAS Journal of Scientific Innovations*, *6*(1), 84-108.

$$\left.\begin{aligned}
S_p(t) &= \frac{\Phi_p{}^{\alpha}}{\mu_p{}^{\alpha}} + \left(S_p(0) - \frac{\Phi_p{}^{\alpha}}{\mu_p{}^{\alpha}} \right) E_{\alpha,1}\left(\mu_p{}^{\alpha} t^{\alpha}\right) > 0, \\
E_p(t) &= E_p(0) E_{\alpha,1}\left(-\left((1-a^{\alpha})\gamma^{\alpha} + a^{\alpha}\gamma^{\alpha} + \mu_p{}^{\alpha}\right)t^{\alpha}\right) > 0, \\
I_{AP}(t) &= I_{AP}(0) E_{\alpha,1}\left(-\left((1-b^{\alpha})\beta^{\alpha} + b^{\alpha}\beta^{\alpha} + \mu_p{}^{\alpha}\right)t^{\alpha}\right) > 0, \\
I_{SP}(t) &= I_{SP}(0) E_{\alpha,1}\left(-\left(\tau^{\alpha} + \mu_p{}^{\alpha} + \delta_p{}^{\alpha}\right)t^{\alpha}\right) > 0, \\
T_{SP}(t) &= T_{SP}(0) E_{\alpha,1}\left(-\left(\sigma^{\alpha} + \mu_p{}^{\alpha}\right)t^{\alpha}\right) > 0, \\
R_P(t) &= R_P(0) E_{\alpha,1}\left(-\mu_p{}^{\alpha} t^{\alpha}\right) > 0, \\
S_v(t) &= \frac{\Phi_v{}^{\alpha}}{\mu_v{}^{\alpha}} + \left(S_v(0) - \frac{\Phi_v{}^{\alpha}}{\mu_v{}^{\alpha}} \right) E_{\alpha,1}\left(\mu_v{}^{\alpha} t^{\alpha}\right) > 0, \\
E_v(t) &= E_v(0) E_{\alpha,1}\left(-\left(\phi^{\alpha} + \mu_v{}^{\alpha}\right)t^{\alpha}\right) > 0, \\
I_v(t) &= I_v(0) E_{\alpha,1}\left(-\mu_v{}^{\alpha} t^{\alpha}\right) > 0,
\end{aligned}\right\}$$

The solutions pertaining to the different compartments exhibit non-negativity. In light of the insights derived from Equations (9), it can be deduced that the ensemble remains positively invariant with respect to temporal progression (t).

Also, in the $E_p - I_{Ap} - I_{SP} - T_{SP} - R_P - E_V - I_v$ plane, the trajectory solution of the developed fractional model (7) is positive, having $t^* > 0$, such that.

$S_p(t^*) = 0,\ E_p(t^*) > 0,\ I_{Ap}(t^*) > 0,\ I_{SP}(t^*) > 0,\ T_{SP}(t^*) > 0,\ R_P(t^*) >,$

$S_v(t^*) = 0,\ E_V(t^*) > 0,\ I_v(t^*) > 0$

and $S_p(t) < S_p(t^*),\ S_v(t) < S_v(t^*)$

On plane

$${}_0^c D_\beta^\alpha S_p(t)|_{t=t^*} = \Phi_p{}^{\alpha},\ \text{and}\ {}_0^c D_\beta^\alpha S_v(t)|_{t=t^*} = \Phi_v{}^{\alpha}, \tag{10}$$

Now, we apply Caputo fractional derivative mean value theorem, and we have

$$S_p(t) - S_p(t^*) = \frac{1}{\Gamma(\alpha)} \cdot {}_0^c D_\beta^\alpha(t')(t - t^*), t' \in [t^*, t) \tag{11}$$

$$S_v(t) - S_v(t^*) = \frac{1}{\Gamma(\alpha)} \cdot {}_0^c D_\beta^\alpha(t')(t - t^*), t' \in [t^*, t)$$

Finally, we have $S_p(t) > S_p(t^*),\ S_v(t) > S_v(t^*)$ and this contradicts our assumption earlier for $t^* > 0$. So, the susceptible classes $S_p(t)$ and $S_v(t)$ are nonnegative for all time t. Hence, the solution of the fractional derivative is positive for all time t.

2.3.3. Boundedness of the solution

From (7), the total population size is

$$N_p = S_p + E_p + I_{Ap} + I_{SP} + T_{SP} + R_P,$$

$$N_v = S_v + E_V + I_v$$

And the differential equation involving fractional derivatives for the population is given by:

Cite this article as:
Loyinmi, A. C. (2024). A fractional-order model for zika virus transmission dynamics: analysis, control strategies, and simulation insights, *FNAS Journal of Scientific Innovations*, *6*(1), 84-108.

$${}_0^c D_\beta^\alpha N_p = {}_0^c D_\beta^\alpha S_p + {}_0^c D_\beta^\alpha E_p + {}_0^c D_\beta^\alpha I_{Ap} + {}_0^c D_\beta^\alpha I_{SP} + {}_0^c D_\beta^\alpha T_{SP} + {}_0^c D_\beta^\alpha R_P,$$

$${}_0^c D_\beta^\alpha N_v = {}_0^c D_\beta^\alpha S_v + {}_0^c D_\beta^\alpha E_V + {}_0^c D_\beta^\alpha I_v$$

By incorporating the fractional model system of equations delineating human population dynamics from equation (7) into the preceding expression and meticulously executing the elimination procedure, a profound outcome ensues.

$${}_0^c D_\beta^\alpha N_p = \Phi_p{}^\alpha - \mu_p{}^\alpha N - \delta_p{}^\alpha I_{SP} \tag{12}$$

$${}_0^c D_\beta^\alpha N_v = \Phi_v{}^\alpha - \mu_v{}^\alpha N$$

Theorem 2

The solution of the fractional model (7) is feasible at $t > 0$ if they enter the region $D = \{S_p, E_p, I_{Ap}, I_{SP}, T_{SP}, R_P, S_v, E_V, I_v\} \in R^9$.

Proof

Demonstrating the constrained nature of the human population's solution, we revisit equation (9) and employ the Laplace transform on both sides of the equation.

$${}_0^c D_\beta^\alpha N_p = \Phi_p{}^\alpha - \mu_p{}^\alpha N - \delta_p{}^\alpha I_{SP}$$

at disease-free, we have the equation to be

$${}_0^c D_\beta^\alpha N_p = \Phi_p{}^\alpha - \mu_p{}^\alpha N \tag{13}$$

Re-arrange the equation above we have,

$${}_0^c D_\beta^\alpha N_p + \mu_p{}^\alpha N = \Phi_p{}^\alpha$$

Utilizing the Laplace transformation methodology, we observe (14)

$$L\left\{{}_0^c D_\beta^\alpha N_p\right\}(S) + \mu_p{}^\alpha L\{N\}(S) = L\left\{\Phi_p{}^\alpha\right\}(S)$$

Following equation (3), the Laplace transform for the Caputo fractional derivate for the above equation is given as

$$S^\alpha \psi - \sum_{n=0}^{m-1} S^{\alpha-n-1} N^n(0) + \mu_p{}^\alpha \psi = \frac{\Phi_p{}^\alpha}{S} \qquad \text{where } L\{N\}(S) = \psi(S) = \psi$$

For $m = 0, 0 < \alpha < 1$, the equation becomes

$$S^\alpha \psi - \sum_{n=0}^{0} S^{\alpha-n-1} N^n(0) + \mu_p{}^\alpha \psi = \frac{\Phi_p{}^\alpha}{S}$$

Now, applying summation property, we have

$$S^\alpha \hat{\lambda} - S^{\alpha-1} N^n(0) + \mu_p{}^\alpha \psi = \frac{\Phi_p{}^\alpha}{S} \tag{15}$$

Then, making $\hat{\lambda}$ the subject of the above equation, we have

$$\psi = \frac{\Phi_p{}^\alpha S^{-1}}{S^\alpha + \mu_p{}^\alpha} + \frac{S^{\alpha-1}}{S^\alpha + \mu_p{}^\alpha} N(0) \tag{16}$$

Utilizing the inverse Laplace transformation on both sides of the aforementioned equation yields the following outcome.

$$L^{-1}\{\psi\} = \Phi_p{}^\alpha L^{-1}\left\{\frac{S^{-1}}{S^\alpha + \mu_p{}^\alpha}\right\} + N(0) L^{-1}\left\{\frac{S^{\alpha-1}}{S^\alpha + \mu_p{}^\alpha}\right\} \tag{17}$$

Applying the inverse Laplace transform and Mittage-Liffler function as in equation (5), we have

Cite this article as:
Loyinmi, A. C. (2024). A fractional-order model for zika virus transmission dynamics: analysis, control strategies, and simulation insights, *FNAS Journal of Scientific Innovations*, *6*(1), 84-108.

$$N(t)=\pi^{\alpha}\left(t^{\alpha+1-1}E_{\alpha,\alpha+1}\left(-{\mu_p}^{\alpha}t^{\alpha}\right)\right)+N(0)\left(t^{1-1}E_{\alpha,1}\left(-{\mu_p}^{\alpha}t^{\alpha}\right)\right) \tag{18}$$

Now, we apply definition 2.4, The Mittage-Liffler function as in equation (4), we have

$$N(t)={\Phi_p}^{\alpha}t^{\alpha}\left(\frac{1}{-{\mu_p}^{\alpha}t^{\alpha}}E_{\alpha,1}\left(-{\mu_p}^{\alpha}t^{\alpha}\right)-\frac{1}{-{\mu_p}^{\alpha}t^{\alpha}}\sqrt{1}\right)+N(0)E_{\alpha,1}\left(-{\mu_p}^{\alpha}t^{\alpha}\right) \tag{19}$$

By simplification, we have

$$N(t)\le\frac{{\Phi_p}^{\alpha}}{{\mu_p}^{\alpha}}+\left(N(0)-\frac{\pi^{\alpha}}{{\mu_p}^{\alpha}}\right)E_{\alpha,1}\left(-{\mu_p}^{\alpha}t^{\alpha}\right)$$

Finally,

$$\lim_{t\to\infty}N(t)\le\frac{{\Phi_p}^{\alpha}}{{\mu_p}^{\alpha}} \tag{20}$$

Similarly, demonstrating the constrained nature of the vector population's solution, we revisit equation (9) and follow the same procedure. So, we have for the vector population;

$$\lim_{t\to\infty}N(t)\le\frac{{\Phi_v}^{\alpha}}{{\mu_v}^{\alpha}}$$

Existence and Uniqueness of the system

Prior to affirming the presence and singular efficacy of the Zıka Vırus remedy, it is imperative to initially delineate the core functions as per the fractional derivative model (7), thereby establishing the fundamental basis for our demonstration.

$$\left.\begin{aligned}
\Delta_1&={\Phi_p}^{\alpha}-\left({\omega_p}^{\alpha}+{\mu_p}^{\alpha}\right)S_p\\
\Delta_2&={\omega_p}^{\alpha}S_p-\left(\left(1-a^{\alpha}\right)\gamma^{\alpha}+a^{\alpha}\gamma^{\alpha}+{\mu_p}^{\alpha}\right)E_p\\
\Delta_3&=\left(1-a\right)\gamma^{\alpha}E_p-\left(\left(1-b^{\alpha}\right)\beta^{\alpha}+b^{\alpha}\beta^{\alpha}+{\mu_p}^{\alpha}\right)I_{AP}\\
\Delta_4&=a^{\alpha}\gamma^{\alpha}E_p+b^{\alpha}\beta^{\alpha}I_{AP}-\left(\tau^{\alpha}+{\mu_p}^{\alpha}+{\delta_p}^{\alpha}\right)I_{SP}\\
\Delta_5&=\tau^{\alpha}I_{SP}-\left(\sigma^{\alpha}+{\mu_p}^{\alpha}\right)T_{SP}\\
\Delta_6&=\left(1-b^{\alpha}\right)\beta^{\alpha}I_{AP}+\sigma^{\alpha}T_{SP}-{\mu_p}^{\alpha}R_P\\
\Delta_7&={\Phi_v}^{\alpha}-\left({\omega_v}^{\alpha}+{\mu_v}^{\alpha}\right)S_v\\
\Delta_8&={\omega_v}^{\alpha}S_v-\left(\phi^{\alpha}+{\mu_v}^{\alpha}\right)E_v\\
\Delta_9&=\phi^{\alpha}E_v-{\mu_v}^{\alpha}I_v
\end{aligned}\right\} \tag{21}$$

Also, Let $Y(t)=\left(S_p,E_p,I_{Ap},I_{SP},T_{SP},R_P,S_v,E_V,I_v\right)^T$

and $V(t,Y(t))=(\eta_i)^T, i=1,2,3,4,5,6,7,8,9.$

So, we can write the model (7) as follows:

$${}_0^cD_{\beta}^{\alpha}Y(t)=\Delta(t,Y(t)),Y(0)=Y_0\ge 0,t\in[0,b],0<\alpha\le 1. \tag{22}$$

In the given expression, condition $L_0\ge 0$ should be considered separately for each component. Problem (22), which is equivalent to model (7), can be defined by integrating the following:

$$Y(t)=Y_0+\frac{1}{\Gamma(\alpha)}\int_0^{\beta}(\beta-b)^{\alpha-1}\Delta(b,Y(b))db. \tag{23}$$

Cite this article as:
Loyinmi, A. C. (2024). A fractional-order model for zika virus transmission dynamics: analysis, control strategies, and simulation insights, *FNAS Journal of Scientific Innovations*, *6*(1), 84-108.

Subsequently, we will examine model (7) using the integral representation provided earlier. In this scenario, let's $\tau = C([0,\kappa];\Re)$ represent the Banach space comprising all continuous functions that are mapping from the interval $(0,\kappa)$ to $\Re$, equipped with the norm.

$$\|L\|_\tau = \sup_{t\in[0,a]}\{|Y(t)|\}, \tag{24}$$

and $|L(t)| = |S_p(t)| + |E_p(t)| + |I_{Ap}(t)| + |I_{SP}(t)| + |T_{SP}(t)| + |R_P(t)| + |S_v(t)| + |E_V(t)| + |I_v(t)|$

Where $S_p, E_p, I_{Ap}, I_{SP}, T_{SP}, R_P, S_v, E_V, I_v$ all belong to $C([0,\kappa];\Re)$.

Also, the operator $L:\tau\to\tau$ is defined by

$$(YL)(t) = L_0 + \frac{1}{\Gamma(\alpha)}\int_0^\beta (\beta-b)^{\alpha-1}\Delta(b,L(b))db. \tag{25}$$

Therefore, the operator Y is properly defined owing to the evident continuity of V.

Theorem 3. Let $\bar{L} = \left(\bar{S_p}, \bar{E_p}, \bar{I_{Ap}}, \bar{I_{SP}}, \bar{T_{SP}}, \bar{R_P}, \bar{S_v}, \bar{E_V}, \bar{I_v}\right)^T$, the function $\Delta = (\Delta_i)^T$ defined above satisfies

$$\left\|\Delta(t,L(t)) - \Delta\left(t,\bar{L}(t)\right)\right\|_\tau \le H_k\left\|L-\bar{L}\right\|_\tau, \text{ for some } H_k > 0.$$

Proof: We have the first component of the kernel Δ to be

$$\Phi_p{}^\alpha - \left((\theta_1 I_{sp} + \theta_2 I_{AP} + \theta_3 I_v) + \mu_p{}^\alpha\right)S_p$$

$$\left|\Delta(t,L(t)) - \Delta\left(t,\bar{L}(t)\right)\right| \tag{26}$$

$$= \left|\theta_1 \bar{I_{sp}}\,\bar{S_p} + \theta_2\,\bar{I_{AP}}\,\bar{S_p} + \theta_3\,\bar{I_v}\,\bar{S_p} - \theta_1 I_{sp}S_p - \theta_2 I_{AP}S_p - \theta_3 I_v S_p + \mu^\alpha{}_p\,\bar{S_p} - \mu^\alpha{}_p S_p\right|$$

Let

$$n_1 = \max\left\{\theta_1\,\bar{S_p}, \theta_1 S_p\right\},\ n_2 = \max\left\{\theta_2\,\bar{S_p}, \theta_2 S_p\right\},\ n_3 = \max\left\{\theta_3\,\bar{S_p}, \theta_3 S_p\right\}$$ then the equation above can be reduced to

$$\left|\Delta(t,L(t)) - \Delta\left(t,\bar{L}(t)\right)\right| \tag{27}$$

$$\le n_1\left|I_{sp} - \bar{I_{sp}}\right| + n_2\left|I_{AP} - \bar{I_{AP}}\right| + n_3\left|I_v - \bar{I_v}\right| + \mu_p^\alpha\left|S_p - \bar{S_p}\right|$$

$$\le m_1\left(\left|I_{sp} - \bar{I_{sp}}\right| + n_2\left|I_{AP} - \bar{I_{AP}}\right| + \left|I_v - \bar{I_v}\right| + \left|S_p - \bar{S_p}\right|\right)$$

Where $m_1 = \max\{n_1, n_2, n_{3,}\mu_p^\alpha\}$.

So,

$$\left|\Delta(t,L(t)) - \Delta\left(t,\bar{L}(t)\right)\right| \tag{28}$$

$$\le m_1\left(\left|I_{sp} - \bar{I_{sp}}\right| + n_2\left|I_{AP} - \bar{I_{AP}}\right| + \left|I_v - \bar{I_v}\right| + \left|S_p - \bar{S_p}\right|\right),$$

Similarly, the rest can be demonstrated in a comparable manner. As a result, we can infer that

Cite this article as:
Loyinmi, A. C. (2024). A fractional-order model for zika virus transmission dynamics: analysis, control strategies, and simulation insights, *FNAS Journal of Scientific Innovations*, *6*(1), 84-108.

$$\left\|\Delta(t,L(t))-\Delta\left(t,\bar{L}(t)\right)\right\|_{\tau} \le m_l \left\|L-\bar{L}\right\|_{\tau},$$

for $m_l = m_1 + m_2 + m_3 + m_4 + m_5 + m_6 + m_7 + m_8 + m_9$

Theorem 4: If the condition $\mathrm{P} = \dfrac{\Phi_p{}^{\alpha}}{\Gamma(\alpha+1)}$ is satisfied by the preceding theorem, and condition $\mathrm{P}m_i < 1$ holds, then there exists a sole solution to model (7) on domain $\left(0, \Phi_p{}^{\alpha}\right)$ that maintains uniform Lyapunov stability.

Proof: The function $\mathrm{P}\left[0, \Phi_p{}^{\alpha}\right] \times \Re_+^6 \to \Re_+^6$ is evidently continuous within its specified domain. Consequently, we demonstrate the existence of the solution.

To establish uniqueness, we employ the Banach contraction mapping theorem on the operator Y defined earlier. Subsequently, we demonstrate that Y functions as both a self-map and a contraction.

By definition, $\sup_{t\in[0,a]}\|\mathrm{P}(t,o)\| = \Phi_p{}^{\alpha}$,

Then, we define $l > \|L_0\| + \Theta\Phi_p{}^{\alpha}/1-\Theta m_i$ and a close convex set $H_l = \left\{L \in \tau : \|L\|_{\tau} \le l\right\}$.

Thus, with regard to the self-mapping attribute, it suffices to demonstrate that $YH_l \subset H_l$. So let $Y \in H_l$,

Then

$$\|YL\|_{\tau} = \sup_{t\in\left[0,\Phi_p{}^{\alpha}\right]}\left\{\left|L_0 + \frac{1}{\Gamma(\alpha)}\int_0^{\beta}(\beta-b)^{\alpha-1}\mathrm{P}(b,L(b))db\right|\right\}, \tag{29}$$

$$\le |L_0| + \frac{1}{\Gamma(\alpha)}\sup_{t\in\left[0,\Phi_p{}^{\alpha}\right]}\left\{\int_0^{\beta}(\beta-b)^{\alpha-1}\left(|\mathrm{P}(b,L(b)) - \mathrm{P}(b,0)| + |\mathrm{P}(b,0)|\right)db\right\},$$

$$\le |L_0| + \frac{1}{\Gamma(\alpha)}\sup_{t\in\left[0,\Phi_p{}^{\alpha}\right]}\left\{\int_0^{\beta}(\beta-b)^{\alpha-1}\left(\|\mathrm{P}(b,L(b)) - H(b,0)\|_{\tau} + \|\mathrm{P}(b,0)\|\right)db\right\},$$

$$\le |L_0| + \frac{m_l\|L\|_{\tau}\, l + \Phi_p{}^{\alpha}}{\Gamma(\alpha)}\sup_{t\in\left[0,\Phi_p{}^{\alpha}\right]}\left\{\int_0^{\beta}(\beta-b)^{\alpha-1}db\right\},$$

$$\le |L_0| + \frac{m_l l + \Phi_p{}^{\alpha}}{\Gamma(\alpha)}\sup_{t\in\left[0,\Phi_p{}^{\alpha}\right]}\left\{\int_0^{\beta}(\beta-b)^{\alpha-1}db\right\},$$

$$= |L_0| + \frac{m_l l + \Phi_p{}^{\alpha}}{\Gamma(\alpha+1)}\alpha,$$

$$= |L_0| + \mathrm{P}\left(m_l l + \Phi_p{}^{\alpha}\right) \le l. \tag{30}$$

Consequently, it is observed that operators $YL \subseteq H_l$ and Y exhibit characteristics of self-maps within the context.

Subsequently, we establish the contraction property of operator Y. Assuming operators L and $\bar{L}$ conform to the abbreviated dynamical system, the application of the aforementioned theorem result yields the following.

$$\left\|YL - Y\bar{L}\right\|_{\tau} = \sup_{t\in\left[0,\Phi_p{}^{\alpha}\right]}\left\{\left|(YL)(t) - \left(Y\bar{L}\right)(t)\right|\right\}, \tag{31}$$

$$= \frac{1}{\Gamma(\alpha)}\sup_{t\in\left[0,\Phi_p{}^{\alpha}\right]}\left\{\int_0^{\beta}(\beta-b)^{\alpha-1}\left|\mathrm{P}(b,L(b)) - \mathrm{P}\left(b,\bar{L}(b)\right)\right|db\right\},$$

Cite this article as:
Loyinmi, A. C. (2024). A fractional-order model for zika virus transmission dynamics: analysis, control strategies, and simulation insights, *FNAS Journal of Scientific Innovations*, *6*(1), 84-108.

$$\leq \frac{m_l}{\Gamma(\alpha)} \sup_{t\in[0,\Phi_p{}^{\alpha}]} \left\{ \int_0^{\beta} (\beta - b)^{\alpha-1} \left| L(b) - \bar{L}(b) \right| db \right\},$$
$$\leq \mathrm{P} m_l \left\| L(b) - \bar{L}(b) \right\|_{\alpha}. \tag{32}$$

Therefore, if $\mathrm{P}m_l < 1$ then Y acts as a contraction mapping. According to the Banach contraction mapping principle, Y possesses a unique fixed point on $\left[0, \Phi_p{}^{\alpha}\right]$, serving as a solution to model (7). Additionally, the uniform Lyapunov stability of the solutions ensues.

Basic Reproduction Number

We derive the fundamental reproductive rate of model (7) employing the methodology introduced by Diekmann and Heesterbeek, known as the next-generation matrix approach in epidemiological analysis. By applying this technique, $R^f = \rho(UV^{-1})$, the expressions for the novel infection components, denoted as U, and the transition components, denoted as V, within model (7) are deduced.

$$V = \begin{pmatrix} \left((1-a^{\alpha})\gamma^{\alpha} + a^{\alpha}\gamma^{\alpha} + \mu_p{}^{\alpha}\right)E_p \\ -(1-a)\gamma^{\alpha}E_p + \left((1-b^{\alpha})\beta^{\alpha} + b^{\alpha}\beta^{\alpha} + \mu_p{}^{\alpha}\right)I_{AP} \\ -a^{\alpha}\gamma^{\alpha}E_p - b^{\alpha}\beta^{\alpha}I_{AP} + \left(\tau^{\alpha} + \mu_p{}^{\alpha} + \delta_p{}^{\alpha}\right)I_{SP} \\ \left(\phi^{\alpha} + \mu_v{}^{\alpha}\right)E_v \\ -\phi^{\alpha}E_v + \mu_v{}^{\alpha}I_v \end{pmatrix}$$

$$U = \begin{pmatrix} \left(\theta_1 I_{sp} + \theta_2 I_{AP} + \theta_3 I_v\right)S_p \\ 0 \\ 0 \\ \left(\theta_4 I_{sp} + \theta_5 I_{AP}\right)S_v \\ 0 \end{pmatrix} \tag{33}$$

$$V = \begin{pmatrix} \left((1-a^{\alpha})\gamma^{\alpha} + a^{\alpha}\gamma^{\alpha} + \mu_p{}^{\alpha}\right)E_p \\ -(1-a)\gamma^{\alpha}E_p + \left((1-b^{\alpha})\beta^{\alpha} + b^{\alpha}\beta^{\alpha} + \mu_p{}^{\alpha}\right)I_{AP} \\ -a^{\alpha}\gamma^{\alpha}E_p - b^{\alpha}\beta^{\alpha}I_{AP} + \left(\tau^{\alpha} + \mu_p{}^{\alpha} + \delta_p{}^{\alpha}\right)I_{SP} \\ \left(\phi^{\alpha} + \mu_v{}^{\alpha}\right)E_v \\ -\phi^{\alpha}E_v + \mu_v{}^{\alpha}I_v \end{pmatrix} \tag{34}$$

$$U = \begin{bmatrix} 0 & \theta_1 S_p & \theta_2 S_p & 0 & \theta_3 S_p \\ 0 & 0 & 0 & 0 & 0 \\ 0 & 0 & 0 & 0 & 0 \\ 0 & \theta_4 S_V & \theta_5 S_V & 0 & 0 \\ 0 & 0 & 0 & 0 & 0 \end{bmatrix} \tag{35}$$

Cite this article as:
Loyinmi, A. C. (2024). A fractional-order model for zika virus transmission dynamics: analysis, control strategies, and simulation insights, *FNAS Journal of Scientific Innovations*, *6*(1), 84-108.

$$V=\begin{bmatrix} \left(\left(1-a^{\alpha}\right)\gamma^{\alpha}+a^{\alpha}\gamma^{\alpha}+{\mu_p}^{\alpha}\right) & 0 & 0 & 0 & 0 \\ -\left(1-a\right)\gamma^{\alpha} & \left(\left(1-b^{\alpha}\right)\beta^{\alpha}+b^{\alpha}\beta^{\alpha}+{\mu_p}^{\alpha}\right) & 0 & 0 & 0 \\ -a^{\alpha}\gamma^{\alpha} & -b^{\alpha}\beta^{\alpha} & \left(\tau^{\alpha}+{\mu_p}^{\alpha}+{\delta_p}^{\alpha}\right) & 0 & 0 \\ 0 & 0 & 0 & \left(\phi^{\alpha}+{\mu_v}^{\alpha}\right) & 0 \\ 0 & 0 & 0 & -\phi^{\alpha} & {\mu_v}^{\alpha} \end{bmatrix}$$

Let $p=\left(1-a^{\alpha}\right)\gamma^{\alpha}+a^{\alpha}\gamma^{\alpha}+{\mu_p}^{\alpha}$; $q=-\left(1-a\right)\gamma^{\alpha}$; $r=-a^{\alpha}\gamma^{\alpha}$; $s=\left(\phi^{\alpha}+{\mu_v}^{\alpha}\right)$

$t=\left(\left(1-b^{\alpha}\right)\beta^{\alpha}+b^{\alpha}\beta^{\alpha}+{\mu_p}^{\alpha}\right)$ $u=-b^{\alpha}\beta^{\alpha}$ $v=\left(\tau^{\alpha}+{\mu_p}^{\alpha}+{\delta_p}^{\alpha}\right)$ $w=-\phi^{\alpha}$ $x={\mu_v}^{\alpha}$

Then,

$$V=\begin{bmatrix} p & 0 & 0 & 0 & 0 \\ q & t & 0 & 0 & 0 \\ r & u & v & 0 & 0 \\ 0 & 0 & 0 & s & 0 \\ 0 & 0 & 0 & w & x \end{bmatrix} \tag{36}$$

And

$$V^{-1}=\begin{bmatrix} \frac{1}{p} & 0 & 0 & 0 & 0 \\ \frac{-q}{pt} & \frac{1}{t} & 0 & 0 & 0 \\ \frac{qu-tr}{ptv} & -\frac{u}{tv} & \frac{1}{v} & 0 & 0 \\ 0 & 0 & 0 & \frac{1}{s} & 0 \\ 0 & 0 & 0 & -\frac{w}{sx} & \frac{1}{x} \end{bmatrix} \tag{37}$$

So for UV^{-1}, we have the fundamental reproductive rate corresponds to the spectral radius of the matrix representing the propagation of infections to subsequent generations. Thus, from above, we obtain the expression for R^{f}, where ${R_H}^{f}$ represent the reproduction for the human population and ${R_V}^{f}$ denote the reproduction ration for the vector population.

$${R_H}^{f}=\frac{S_p}{\left(\gamma^{\alpha}+{\mu_p}^{\alpha}\right)\left(\beta^{\alpha}+{\mu_p}^{\alpha}\right)}\left(\theta_1\left(1-a\right)\gamma^{\alpha}+\frac{\theta_2\left(\left(1-a\right)\gamma^{\alpha}b^{\alpha}\beta^{\alpha}+\left(\beta^{\alpha}+{\mu_p}^{\alpha}\right)a^{\alpha}\gamma^{\alpha}\right)}{\left(\tau^{\alpha}+{\mu_p}^{\alpha}+{\delta_p}^{\alpha}\right)}\right)$$

Also ${R_V}^{f}=\frac{S_v}{\left(\gamma^{\alpha}+{\mu_p}^{\alpha}\right)\left(\beta^{\alpha}+{\mu_p}^{\alpha}\right)}\left(\theta_4\left(1-a\right)\gamma^{\alpha}+\frac{\theta_5\left(\left(1-a\right)\gamma^{\alpha}b^{\alpha}\beta^{\alpha}+\left(\beta^{\alpha}+{\mu_p}^{\alpha}\right)a^{\alpha}\gamma^{\alpha}\right)}{\left(\tau^{\alpha}+{\mu_p}^{\alpha}+{\delta_p}^{\alpha}\right)}\right)$

Analysis of the fractional model

Disease-Free Equilibrium (DFE)

The state of disease absence, $\left(E_D^{f}\right)$, denoted as the disease-free equilibrium within the fractional model (7), signifies a stable condition wherein the disease undergoes eradication. Through the establishment of steady-state conditions by equating the pertinent variables associated with the disease to zero, model (7) generates the subsequent manifestation for the disease-free equilibrium.

$$E^{FD}=\left(\frac{{\Phi_p}^{\alpha}}{{\mu_p}^{\alpha}},0,0,0,0,0,0,\frac{{\Phi_v}^{\alpha}}{{\mu_v}^{\alpha}},0\right) \tag{39}$$

Now, by setting the state variables associated with the disease to zero and solving, we obtain the following:

Cite this article as:
Loyinmi, A. C. (2024). A fractional-order model for zika virus transmission dynamics: analysis, control strategies, and simulation insights, *FNAS Journal of Scientific Innovations*, *6*(1), 84-108.

$$\left.\begin{aligned}
0 &= {\Phi_p}^{\alpha} - \left({\omega_p}^{\alpha} + {\mu_p}^{\alpha}\right)S_p \\
0 &= {\omega_p}^{\alpha} S_p - \left(\left(1-a^{\alpha}\right)\gamma^{\alpha} + a^{\alpha}\gamma^{\alpha} + {\mu_p}^{\alpha}\right)E_p \\
0 &= \left(1-a\right)\gamma^{\alpha} E_p - \left(\left(1-b^{\alpha}\right)\beta^{\alpha} + b^{\alpha}\beta^{\alpha} + {\mu_p}^{\alpha}\right)I_{AP} \\
0 &= a^{\alpha}\gamma^{\alpha} E_p + b^{\alpha}\beta^{\alpha} I_{AP} - \left(\tau^{\alpha} + {\mu_p}^{\alpha} + {\delta_p}^{\alpha}\right)I_{SP} \\
0 &= \tau^{\alpha} I_{SP} - \left(\sigma^{\alpha} + {\mu_p}^{\alpha}\right)T_{SP} \\
0 &= \left(1-b^{\alpha}\right)\beta^{\alpha} I_{AP} + \sigma^{\alpha} T_{SP} - {\mu_p}^{\alpha} R_P \\
0 &= {\Phi_v}^{\alpha} - \left({\omega_v}^{\alpha} + {\mu_v}^{\alpha}\right)S_v \\
0 &= {\omega_v}^{\alpha} S_v - \left(\phi^{\alpha} + {\mu_v}^{\alpha}\right)E_v \\
0 &= \phi^{\alpha} E_v - {\mu_v}^{\alpha} I_v
\end{aligned}\right\} \tag{40}$$

Furthermore, at the point where $E_p, I_{Ap}, I_{SP}, T_{SP}, R_P, E_V$, and I_v vanish, we derive:

$${S_p}^0 = \frac{{\Phi_p}^{\alpha}}{{\mu_p}^{\alpha}} \text{ and } {S_v}^0 = \frac{{\Phi_v}^{\alpha}}{{\mu_v}^{\alpha}} \tag{41}$$

Therefore, the determination of the equilibrium devoid of disease within the fractional model necessitates the utilization of basic mathematical computations, as delineated subsequently:

$$E^{FD} = \left(\frac{{\Phi_p}^{\alpha}}{{\mu_p}^{\alpha}}, 0, 0, 0, 0, 0, 0, \frac{{\Phi_v}^{\alpha}}{{\mu_v}^{\alpha}}, 0\right)$$

Stability Analysis of the DFE

Theorem 4: The state of disease absence within the system $E^{FD} = \left(\frac{{\Phi_p}^{\alpha}}{{\mu_p}^{\alpha}}, 0, 0, 0, 0, 0, 0, \frac{{\Phi_v}^{\alpha}}{{\mu_v}^{\alpha}}, 0\right)$ exhibits asymptotic stability when all eigenvalues of the Jacobian matrix associated with the system's dynamics are characterized by negativity.

Proof:

In order to substantiate the aforementioned theorem, we undertake the computation of the Jacobian Matrix pertaining to system (7) at the Disease-Free Equilibrium (DFE) point, $E^{FD} = \left(\frac{{\Phi_p}^{\alpha}}{{\mu_p}^{\alpha}}, 0, 0, 0, 0, 0, 0, \frac{{\Phi_v}^{\alpha}}{{\mu_v}^{\alpha}}, 0\right)$, followed by the assessment of the system's eigenvalues.

The Jacobian Matrix $J\left(S_p, E_p, I_{Ap}, I_{SP}, T_{SP}, R_P, S_v, E_V, I_v\right)$ of the system at DFE, is given as:

$$J = \begin{bmatrix}
-{\mu_p}^{\alpha} & 0 & -{\theta_2}^{\alpha} S_P & -{\theta_1}^{\alpha} S_P & 0 & 0 & 0 & 0 & -{\theta_3}^{\alpha} S_P \\
0 & -\left(\gamma^{\alpha} + {\mu_p}^{\alpha}\right) & {\theta_2}^{\alpha} S_P & {\theta_1}^{\alpha} S_P & 0 & 0 & 0 & 0 & {\theta_3}^{\alpha} S_P \\
0 & \left(1-a\right)\gamma^{\alpha} & -\left(\beta^{\alpha} + {\mu_p}^{\alpha}\right) & 0 & 0 & 0 & 0 & 0 & 0 \\
0 & a^{\alpha}\gamma^{\alpha} & b^{\alpha}\beta^{\alpha} & -\left(\tau^{\alpha} + {\mu_p}^{\alpha} + {\delta_p}^{\alpha}\right) & 0 & 0 & 0 & 0 & 0 \\
0 & 0 & 0 & \tau^{\alpha} & -\left(\sigma^{\alpha} + {\mu_p}^{\alpha}\right) & 0 & 0 & 0 & 0 \\
0 & 0 & 0 & \left(1-b^{\alpha}\right)\beta^{\alpha} & \sigma^{\alpha} & -{\mu_p}^{\alpha} & 0 & 0 & 0 \\
0 & 0 & -\theta_5 S_v & -\theta_4 S_v & 0 & 0 & -{\mu_v}^{\alpha} & 0 & 0 \\
0 & 0 & \theta_5 S_v & \theta_4 S_v & 0 & 0 & 0 & -\left(\phi^{\alpha} + {\mu_v}^{\alpha}\right) & 0 \\
0 & 0 & 0 & 0 & 0 & 0 & 0 & \phi^{\alpha} & -{\mu_v}^{\alpha}
\end{bmatrix} \tag{42}$$

In the process of computing eigenvalues, we adhere to the following steps:

Cite this article as:
Loyinmi, A. C. (2024). A fractional-order model for zika virus transmission dynamics: analysis, control strategies, and simulation insights, *FNAS Journal of Scientific Innovations*, *6*(1), 84-108.

$$|J-\lambda| = \begin{vmatrix} -\mu_p{}^{\alpha}-\lambda & 0 & -\theta_2{}^{\alpha}S_p & -\theta_1{}^{\alpha}S_p & 0 & 0 & 0 & 0 & -\theta_3{}^{\alpha}S_p \\ 0 & -\left(\gamma^{\alpha}+\mu_p{}^{\alpha}\right)-\lambda & \theta_2{}^{\alpha}S_p & \theta_1{}^{\alpha}S_p & 0 & 0 & 0 & 0 & \theta_3{}^{\alpha}S_p \\ 0 & (1-a)\gamma^{\alpha} & -\left(\beta^{\alpha}+\mu_p{}^{\alpha}\right)-\lambda & 0 & 0 & 0 & 0 & 0 & 0 \\ 0 & a^{\alpha}\gamma^{\alpha} & b^{\alpha}\beta^{\alpha} & -\left(\tau^{\alpha}+\mu_p{}^{\alpha}+\delta_p{}^{\alpha}\right)-\lambda & 0 & 0 & 0 & 0 & 0 \\ 0 & 0 & 0 & \tau^{\alpha} & -\left(\sigma^{\alpha}+\mu_p{}^{\alpha}\right)-\lambda & 0 & 0 & 0 & 0 \\ 0 & 0 & 0 & (1-b^{\alpha})\beta^{\alpha} & \sigma^{\alpha} & -\mu_p{}^{\alpha}-\lambda & 0 & 0 & 0 \\ 0 & 0 & -\theta_5 S_v & -\theta_4 S_v & 0 & 0 & -\mu_v{}^{\alpha}-\lambda & 0 & 0 \\ 0 & 0 & \theta_5 S_v & \theta_4 S_v & 0 & 0 & 0 & -\left(\phi^{\alpha}+\mu_v{}^{\alpha}\right)-\lambda & 0 \\ 0 & 0 & 0 & 0 & 0 & 0 & 0 & \phi^{\alpha} & -\mu_v{}^{\alpha}-\lambda \end{vmatrix} \tag{43}$$

Clearly, the diagonal entries in the provided matrix represent the eigenvalues of matrix J. It is evident that these eigenvalues are purely real and devoid of any imaginary components. The importance lies in the signs of these eigenvalues, which are essential for evaluating the stability of the Disease-Free Equilibrium (DFE). In this specific context, all eigenvalues demonstrate negative real parts, confirming the local asymptotic stability of the rotavirus at the DFE.

Infection Persistence Equilibrium

Theorem 6.

In the fractional derivative model (7), the existence of the endemic equilibrium denotes a condition wherein diseases endure within the population. Accordingly, the formulation for the endemic equilibrium can be delineated as follows:

$$E_f = \left(S_p{}^{*}, E_p{}^{*}, I_{Ap}{}^{*}, I_{SP}{}^{*}, T_{SP}{}^{*}, R_P{}^{*}, S_v{}^{*}, E_V{}^{*}, I_v{}^{*}\right),$$

Where $S_p{}^{*}, E_p{}^{*}, I_{Ap}{}^{*}, I_{SP}{}^{*}, T_{SP}{}^{*}, R_P{}^{*}, S_v{}^{*}, E_V{}^{*}, I_v{}^{*}$ are determined by solving the following equation

$$\left.\begin{aligned}
{}_0^cD_t^{\alpha}S_p &= \Phi_p{}^{\alpha} - \left(\left(1-k_1{}^{\alpha}\right)\left(\theta_1{}^{\alpha}I_{sp} + \theta_2{}^{\alpha}I_{AP} + \theta_3{}^{\alpha}I_v\right) + \mu_p{}^{\alpha}\right)S_p \\
{}_0^cD_t^{\alpha}E_p &= \left(1-k_1{}^{\alpha}\right)\left(\theta_1{}^{\alpha}I_{sp} + \theta_2{}^{\alpha}I_{AP} + \theta_3{}^{\alpha}I_v\right)S_p - \left(\left(1-a^{\alpha}\right)\gamma^{\alpha} + a^{\alpha}\gamma^{\alpha} + \mu_p{}^{\alpha}\right)E_p \\
{}_0^cD_t^{\alpha}I_{AP} &= (1-a)\gamma^{\alpha}E_p - \left(\left(1-b^{\alpha}\right)\beta^{\alpha} + b^{\alpha}\beta^{\alpha} + \mu_p{}^{\alpha}\right)I_{AP} \\
{}_0^cD_t^{\alpha}I_{SP} &= a^{\alpha}\gamma^{\alpha}E_p + b^{\alpha}\beta^{\alpha}I_{AP} - \left(k_2{}^{\alpha} + \mu_p{}^{\alpha} + \delta_p{}^{\alpha}\right)I_{SP} \\
{}_0^cD_t^{\alpha}T_{SP} &= k_2{}^{\alpha}I_{SP} - \left(\sigma^{\alpha} + \mu_p{}^{\alpha}\right)T_{SP} \\
{}_0^cD_t^{\alpha}R_P &= \left(1-b^{\alpha}\right)\beta^{\alpha}I_{AP} + \sigma^{\alpha}T_{SP} - \mu_p{}^{\alpha}R_P \\
{}_0^cD_t^{\alpha}S_v &= \Phi_v{}^{\alpha} - \left(\left(1-k_3{}^{\alpha}\right)\left(\theta_4{}^{\alpha}I_{sp} + \theta_5{}^{\alpha}I_{AP}\right) + \mu_v{}^{\alpha}\right)S_V \\
{}_0^cD_t^{\alpha}E_v &= \left(1-k_3{}^{\alpha}\right)\left(\theta_4{}^{\alpha}I_{sp} + \theta_5{}^{\alpha}I_{AP}\right)S_v - \left(\phi^{\alpha} + \mu_v{}^{\alpha}\right)E_v \\
{}_0^cD_t^{\alpha}I_v &= \phi^{\alpha}E_v - \mu_v{}^{\alpha}I_v
\end{aligned}\right\} \tag{50}$$

Additionally, by employing a numerical simulation methodology, we attain the endemic equilibrium through a specified problem-solving strategy.

Fractional optimal control strategies

Here are pivotal elements of fractional optimal control for Zika Virus: we alleviate the transmission rate of the human compartments through $(1-k_1)$, where k_1 symbolizes individual vaccination, k_2 represents the effort of treatment of symptomatic individuals. Also, we alleviate the transmission rate of the vector population through $(1-k_3)$, where k_3 symbolizes environmental management (source reduction, water management and urban planning). Based on these premises, the ensuing collection of novel Caputo fractional derivatives equations is formulated:

Cite this article as:
Loyinmi, A. C. (2024). A fractional-order model for zika virus transmission dynamics: analysis, control strategies, and simulation insights, *FNAS Journal of Scientific Innovations*, *6*(1), 84-108.

$$\left.\begin{aligned}
{}_0^cD_t^{\alpha}S_p &= \Phi_p{}^{\alpha} - \left(\left(1-k_1{}^{\alpha}\right)\left(\theta_1{}^{\alpha}I_{sp}+\theta_2{}^{\alpha}I_{AP}+\theta_3{}^{\alpha}I_v\right)+\mu_p{}^{\alpha}\right)S_p\\
{}_0^cD_t^{\alpha}E_p &= \left(1-k_1{}^{\alpha}\right)\left(\theta_1{}^{\alpha}I_{sp}+\theta_2{}^{\alpha}I_{AP}+\theta_3{}^{\alpha}I_v\right)S_p - \left(\left(1-a^{\alpha}\right)\gamma^{\alpha}+a^{\alpha}\gamma^{\alpha}+\mu_p{}^{\alpha}\right)E_p\\
{}_0^cD_t^{\alpha}I_{AP} &= (1-a)\gamma^{\alpha}E_p - \left(\left(1-b^{\alpha}\right)\beta^{\alpha}+b^{\alpha}\beta^{\alpha}+\mu_p{}^{\alpha}\right)I_{AP}\\
{}_0^cD_t^{\alpha}I_{SP} &= a^{\alpha}\gamma^{\alpha}E_p+b^{\alpha}\beta^{\alpha}I_{AP} - \left(k_2{}^{\alpha}+\mu_p{}^{\alpha}+\delta_p{}^{\alpha}\right)I_{SP}\\
{}_0^cD_t^{\alpha}T_{SP} &= k_2{}^{\alpha}I_{SP} - \left(\sigma^{\alpha}+\mu_p{}^{\alpha}\right)T_{SP}\\
{}_0^cD_t^{\alpha}R_P &= \left(1-b^{\alpha}\right)\beta^{\alpha}I_{AP}+\sigma^{\alpha}T_{SP} - \mu_p{}^{\alpha}R_P\\
{}_0^cD_t^{\alpha}S_v &= \Phi_v{}^{\alpha} - \left(\left(1-k_3{}^{\alpha}\right)\left(\theta_4{}^{\alpha}I_{sp}+\theta_5{}^{\alpha}I_{AP}\right)+\mu_v{}^{\alpha}\right)S_V\\
{}_0^cD_t^{\alpha}E_v &= \left(1-k_3{}^{\alpha}\right)\left(\theta_4{}^{\alpha}I_{sp}+\theta_5{}^{\alpha}I_{AP}\right)S_v - \left(\phi^{\alpha}+\mu_v{}^{\alpha}\right)E_v\\
{}_0^cD_t^{\alpha}I_v &= \phi^{\alpha}E_v - \mu_v{}^{\alpha}I_v
\end{aligned}\right\} \quad (51)$$

Analysis of the Model Integrating Preventive Interventions

In this section, a framework has been developed that integrate a precise functional, emphasizing its controllability via the implementation of Pontryagin's Maximum Principle. Focusing on the fractional optimal setup outlined in equation system (51), emphasis has been placed on a significant control challenge, elucidated prior to engaging in thorough global optimization. The intricate task of selecting the most effective strategies is encapsulated by the functional objective denoted as H. The overarching predetermined objective involves diminishing the population across all categories, all within a specified timeframe [0, T].

Let $N = \left\{\left(k_1, k_2, k_3\right) \in N\right\}$ be Lebesgue measurable on $[0,1]$,

Where $0 \le k_i(t) \le 1 \in [0,1], i = 1,2,3$ (52)

Next, we introduce the target function, G , to be

$$G(k_1,k_2,k_3) = \int_0^T \left(X_1E_v + X_2T_{sp} + X_3E_p + \frac{1}{2}\left(Y_1k_1^2 + Y_2k_2^2 + Y_3k_3^2\right)\right)dt \quad (53)$$

constraint to

$$\left.\begin{aligned}
{}_0^cD_t^{\alpha}S_p &= \Phi_p{}^{\alpha} - \left(\left(1-k_1{}^{\alpha}\right)\left(\theta_1{}^{\alpha}I_{sp}+\theta_2{}^{\alpha}I_{AP}+\theta_3{}^{\alpha}I_v\right)+\mu_p{}^{\alpha}\right)S_p\\
{}_0^cD_t^{\alpha}E_p &= \left(1-k_1{}^{\alpha}\right)\left(\theta_1{}^{\alpha}I_{sp}+\theta_2{}^{\alpha}I_{AP}+\theta_3{}^{\alpha}I_v\right)S_p - \left(\left(1-a^{\alpha}\right)\gamma^{\alpha}+a^{\alpha}\gamma^{\alpha}+\mu_p{}^{\alpha}\right)E_p\\
{}_0^cD_t^{\alpha}I_{AP} &= (1-a)\gamma^{\alpha}E_p - \left(\left(1-b^{\alpha}\right)\beta^{\alpha}+b^{\alpha}\beta^{\alpha}+\mu_p{}^{\alpha}\right)I_{AP}\\
{}_0^cD_t^{\alpha}I_{SP} &= a^{\alpha}\gamma^{\alpha}E_p+b^{\alpha}\beta^{\alpha}I_{AP} - \left(k_2{}^{\alpha}+\mu_p{}^{\alpha}+\delta_p{}^{\alpha}\right)I_{SP}\\
{}_0^cD_t^{\alpha}T_{SP} &= k_2{}^{\alpha}I_{SP} - \left(\sigma^{\alpha}+\mu_p{}^{\alpha}\right)T_{SP}\\
{}_0^cD_t^{\alpha}R_P &= \left(1-b^{\alpha}\right)\beta^{\alpha}I_{AP}+\sigma^{\alpha}T_{SP} - \mu_p{}^{\alpha}R_P\\
{}_0^cD_t^{\alpha}S_v &= \Phi_v{}^{\alpha} - \left(\left(1-k_3{}^{\alpha}\right)\left(\theta_4{}^{\alpha}I_{sp}+\theta_5{}^{\alpha}I_{AP}\right)+\mu_v{}^{\alpha}\right)S_V\\
{}_0^cD_t^{\alpha}E_v &= \left(1-k_3{}^{\alpha}\right)\left(\theta_4{}^{\alpha}I_{sp}+\theta_5{}^{\alpha}I_{AP}\right)S_v - \left(\phi^{\alpha}+\mu_v{}^{\alpha}\right)E_v\\
{}_0^cD_t^{\alpha}I_v &= \phi^{\alpha}E_v - \mu_v{}^{\alpha}I_v
\end{aligned}\right\} \quad (54)$$

The concluding time point is denoted by the parameter T with coefficients aligning with the weight constants attributed to the virus across distinct groups. The focal point in this segment is the reduction of operational costs, as outlined in equation (54). Additionally, our exploration extends to include an examination of the social expenses $Y_1k_1^2, Y_2k_2^2,$ and $Y_3k_3^2$ linked to the described scenario.

Cite this article as:
Loyinmi, A. C. (2024). A fractional-order model for zika virus transmission dynamics: analysis, control strategies, and simulation insights, *FNAS Journal of Scientific Innovations*, *6*(1), 84-108.

To achieve the goal of tackling the control issue, our effort is focused on pinpointing $\left(k_1^*(t), k_2^*(t), k_3^*(t)\right)$, the functionalities in order to

$$G\left(k_1^*(t), k_2^*(t), k_3^*(t)\right) = \min\left\{G(k), (k) \in N\right\} \tag{55}$$

Existence of an Optimal Control Solution

Theorem: Considering equation (51), let $G(k)$ be the optimal control subject to (55), with the initial condition at t=0. The optimal control is given by: $\left(k_1^*(t), k_2^*(t), k_3^*(t)\right)$, such that

$$G\left(k_1^*(t), k_2^*(t), k_3^*(t)\right) = \min\left\{G(k), (k) \in N\right\}$$

Proof: The convex nature of the integrand regarding the control measures G ensures the presence of an optimal solution for control.

Following this, it is crucial to delineate the most effective resolution. The Lagrangian is articulated in the subsequent manner:

$$N_G = X_1 E_v + X_2 T_{sp} + X_3 E_p + \frac{1}{2}\left(Y_1 k_1^2 + Y_2 k_2^2 + Y_3 k_3^2\right)t \tag{56}$$

The Hamiltonian function is given as;

$$\begin{aligned} H_G &= X_1 E_v + X_2 T_{sp} + X_3 E_p + \frac{1}{2}\left(Y_1 k_1^2 + Y_2 k_2^2 + Y_3 k_3^2\right)t \\ &\Pi_{S_p}\left[S_p'\right] + \Pi_{E_p}\left[E_p'\right] + \Pi_{I_{Ap}}\left[I_{Ap}'\right] + \Pi_{I_{Sp}}\left[I_{Sp}'\right] + \Pi_{T_{Sp}}\left[T_{Sp}'\right] \\ &+ \Pi_{R_p}\left[R_p'\right] + \Pi_{S_v}\left[S_v'\right] + \Pi_{E_v}\left[E_v'\right] + \Pi_{I_v}\left[I_v'\right] \end{aligned} \tag{57}$$

and

$$\left.\begin{aligned} {}_0^c D_t^\alpha S_p &= \Phi_p{}^\alpha - \left(\left(1-k_1{}^\alpha\right)\left(\theta_1{}^\alpha I_{sp} + \theta_2{}^\alpha I_{AP} + \theta_3{}^\alpha I_v\right) + \mu_p{}^\alpha\right)S_p \\ {}_0^c D_t^\alpha E_p &= \left(1-k_1{}^\alpha\right)\left(\theta_1{}^\alpha I_{sp} + \theta_2{}^\alpha I_{AP} + \theta_3{}^\alpha I_v\right)S_p - \left(\left(1-a^\alpha\right)\gamma^\alpha + a^\alpha\gamma^\alpha + \mu_p{}^\alpha\right)E_p \\ {}_0^c D_t^\alpha I_{AP} &= (1-a)\gamma^\alpha E_p - \left(\left(1-b^\alpha\right)\beta^\alpha + b^\alpha\beta^\alpha + \mu_p{}^\alpha\right)I_{AP} \\ {}_0^c D_t^\alpha I_{SP} &= a^\alpha\gamma^\alpha E_p + b^\alpha\beta^\alpha I_{AP} - \left(k_2{}^\alpha + \mu_p{}^\alpha + \delta_p{}^\alpha\right)I_{SP} \\ {}_0^c D_t^\alpha T_{SP} &= k_2{}^\alpha I_{SP} - \left(\sigma^\alpha + \mu_p{}^\alpha\right)T_{SP} \\ {}_0^c D_t^\alpha R_P &= \left(1-b^\alpha\right)\beta^\alpha I_{AP} + \sigma^\alpha T_{SP} - \mu_p{}^\alpha R_P \\ {}_0^c D_t^\alpha S_v &= \Phi_v{}^\alpha - \left(\left(1-k_3{}^\alpha\right)\left(\theta_4{}^\alpha I_{sp} + \theta_5{}^\alpha I_{AP}\right) + \mu_v{}^\alpha\right)S_V \\ {}_0^c D_t^\alpha E_v &= \left(1-k_3{}^\alpha\right)\left(\theta_4{}^\alpha I_{sp} + \theta_5{}^\alpha I_{AP}\right)S_v - \left(\phi^\alpha + \mu_v{}^\alpha\right)E_v \\ {}_0^c D_t^\alpha I_v &= \phi^\alpha E_v - \mu_v{}^\alpha I_v \end{aligned}\right\} \tag{58}$$

Provided $\Pi_i, i \in \left\{S_p, E_p, I_{Ap}, I_{SP}, T_{SP}, R_P, S_v, E_V, I_v\right\}$ are discrete and mutually exclusive variables.

We are ready to apply the fundamental prerequisites to the Hamiltonian (H_G) for examination. To uncover the adjunct equation and satisfy the transversality condition, we utilize the Hamiltonian. Through the application of differential processes, we ascertain the values linked to the variables $S_p, E_p, I_{Ap}, I_{SP}, T_{SP}, R_P, S_v, E_V, I_v$ concerning the Hamiltonian. This culminates in the derivation of the adjunct equation, articulated as follows:

$${}_0^c D_t^\alpha S_p = -\frac{\partial H_G}{dS_p} = \Pi_{S_p}\left(\left(1-k_1{}^\alpha\right)\omega_p{}^\alpha + \mu_p{}^\alpha\right) - \Pi_{E_p}\left[\left(1-k_1{}^\alpha\right)\omega_p{}^\alpha S_p\right]\Bigg\}$$

Cite this article as:
Loyinmi, A. C. (2024). A fractional-order model for zika virus transmission dynamics: analysis, control strategies, and simulation insights, *FNAS Journal of Scientific Innovations*, 6(1), 84-108.

$$\left.\begin{aligned} {}_0^cD_t^{\alpha}E_p &= -\frac{\partial H_G}{dE_p} = -X_3 + \Pi_{E_p}\left(\left(1-a^{\alpha}\right)\gamma^{\alpha} + a^{\alpha}\gamma^{\alpha} + {\mu_p}^{\alpha}\right) - \Pi_{I_{AP}}\left[(1-a)\gamma^{\alpha}\right] - \Pi_{I_{SP}}\left[a^{\alpha}\gamma^{\alpha}\right] \\ {}_0^cD_t^{\alpha}I_{AP} &= -\frac{\partial H_G}{dI_{AP}} = \left(\left(1-{k_1}^{\alpha}\right){\theta_2}^{\alpha}\right)S_p\Pi_{S_p} - \left(\left(1-{k_1}^{\alpha}\right){\theta_2}^{\alpha}S_p\right)\Pi_{E_p} + \left(\left(1-b^{\alpha}\right)\beta^{\alpha} + b^{\alpha}\beta^{\alpha} + {\mu_p}^{\alpha}\right)\Pi_{I_{AP}} \\ &\quad - b^{\alpha}\beta^{\alpha}\Pi_{I_{SP}} - \left[\left(1-b^{\alpha}\right)\beta^{\alpha}\right]\Pi_{R_p} + \left[\left(\left(1-{k_3}^{\alpha}\right){\theta_5}^{\alpha}\right)S_V\right]\Pi_{S_V} - \left[\left(1-{k_3}^{\alpha}\right){\theta_5}^{\alpha}S_v\right]\Pi_{E_v} \\ {}_0^cD_t^{\alpha}I_{SP} &= -\frac{\partial H_G}{dI_{SP}} = \left(\left(1-{k_1}^{\alpha}\right){\theta_1}^{\alpha}\right)S_p\Pi_{S_p} - \left(1-{k_1}^{\alpha}\right){\theta_1}^{\alpha}S_p\Pi_{E_p} + \left({k_2}^{\alpha} + {\mu_p}^{\alpha} + {\delta_p}^{\alpha}\right)\Pi_{I_{SP}} \\ &\quad - {k_2}^{\alpha}\Pi_{T_{SP}} + \left(\left(1-{k_3}^{\alpha}\right){\theta_4}^{\alpha}\right)S_V\Pi_{S_V} - \left(\left(1-{k_3}^{\alpha}\right){\theta_4}^{\alpha}\right)S_v\Pi_{E_V} \\ {}_0^cD_t^{\alpha}T_{SP} &= -\frac{\partial H_G}{dT_{SP}} = -X_2 + \left(\sigma^{\alpha} + {\mu_p}^{\alpha}\right)\Pi_{T_{SP}} - \sigma^{\alpha}\Pi_{R_P} \\ {}_0^cD_t^{\alpha}R_P &= -\frac{\partial H_G}{dR_P} = {\mu_p}^{\alpha}\Pi_{R_P} \\ {}_0^cD_t^{\alpha}S_v &= -\frac{\partial H_G}{dS_v} = \left(1-{k_3}^{\alpha}\right)\left({\theta_4}^{\alpha}I_{sp} + {\theta_5}^{\alpha}I_{AP}\right)\Pi_{S_V} - \left(1-{k_3}^{\alpha}\right)\left({\theta_4}^{\alpha}I_{sp} + {\theta_5}^{\alpha}I_{AP}\right)\Pi_{E_V} \\ {}_0^cD_t^{\alpha}E_v &= -\frac{\partial H_G}{dE_v} = -X_1 + \left(\phi^{\alpha} + {\mu_v}^{\alpha}\right)\Pi_{E_v} - \phi^{\alpha}\Pi_{I_v} \\ {}_0^cD_t^{\alpha}I_v &= -\frac{\partial H_G}{dI_v} = \left(\left(1-{k_1}^{\alpha}\right){\theta_3}^{\alpha}\right)S_p\Pi_{S_p} - \left(\left(1-{k_1}^{\alpha}\right){\theta_3}^{\alpha}\right)S_p\Pi_{E_p} + {\mu_v}^{\alpha}\Pi_{I_v} \end{aligned}\right\}$$

Given the transversality conditions, we have:

$$\Pi_i, i \in \left\{S_p, E_p, I_{Ap}, I_{SP}, T_{SP}, R_P, S_v, E_V, I_v\right\}.$$

In the effort to minimize the Hamiltonian, represented as H_G, concerning the optimal control variables, we commence the differentiation process in relation to $k_1, k_2,$ and k_3. This process yields a series of mathematical expressions, subsequently equated to zero to ascertain the optimal configuration of controls. This approach ultimately leads to the derivation of the desired optimal control solution.

Taking (57), thus we have

$$\left.\begin{aligned} \frac{dH_G}{dk_1} &= Y_1k_1 + \left({\theta_1}^{\alpha}I_{sp} + {\theta_2}^{\alpha}I_{AP} + {\theta_3}^{\alpha}I_v\right)S_p\Pi_{S_p} - \left({\theta_1}^{\alpha}I_{sp} + {\theta_2}^{\alpha}I_{AP} + {\theta_3}^{\alpha}I_v\right)S_p\Pi_{E_p} = 0 \\ \frac{dH_G}{dk_2} &= Y_2k_2 - I_{SP}\Pi_{I_{sp}} + I_{SP}\Pi_{T_{sp}} = 0 \\ \frac{dH_G}{dk_3} &= Y_3k_3 + \left({\theta_4}^{\alpha}I_{sp} + {\theta_5}^{\alpha}I_{AP}\right)S_V\Pi_{S_V} - \left({\theta_4}^{\alpha}I_{sp} + {\theta_5}^{\alpha}I_{AP}\right)S_v\Pi_{E_V} = 0 \end{aligned}\right\}$$

We proceed with the process of obtaining the optimal control solution:

Cite this article as:
Loyinmi, A. C. (2024). A fractional-order model for zika virus transmission dynamics: analysis, control strategies, and simulation insights, *FNAS Journal of Scientific Innovations*, *6*(1), 84-108.

$$\left.\begin{aligned} k_1^* &= \frac{\left[\Pi_{E_p} - \Pi_{S_p}\right]\left(\theta_1^{\alpha} I_{sp} + \theta_2^{\alpha} I_{AP} + \theta_3^{\alpha} I_v\right) S_p}{Y_1} \\ k_2^* &= \frac{\left(\Pi_{I_{sp}} - \Pi_{T_{sp}}\right) I_{SP}}{Y_2} \\ k_3^* &= \frac{\left[\Pi_{E_V} - \Pi_{S_V}\right]\left(\theta_4^{\alpha} I_{sp} + \theta_5^{\alpha} I_{AP}\right) S_v}{Y_3} \end{aligned}\right\}$$

Incorporating the boundary parameters, the solution is articulated as follows:

$$\begin{aligned} k_1^* &= \min\left\{1, \max\left\{0, V_1\right\}\right\}; \\ k_2^* &= \min\left\{1, \max\left\{0, V_2\right\}\right\}; \\ k_3^* &= \min\left\{1, \max\left\{0, V_3\right\}\right\}, \end{aligned} \tag{62}$$

with,

$$\left.\begin{aligned} V_1 &= \frac{\left[\Pi_{E_p} - \Pi_{S_p}\right]\left(\theta_1^{\alpha} I_{sp} + \theta_2^{\alpha} I_{AP} + \theta_3^{\alpha} I_v\right) S_p}{Y_1} \\ V_2 &= \frac{\left(\Pi_{I_{sp}} - \Pi_{T_{sp}}\right) I_{SP}}{Y_2} \\ V_3 &= \frac{\left[\Pi_{E_V} - \Pi_{S_V}\right]\left(\theta_4^{\alpha} I_{sp} + \theta_5^{\alpha} I_{AP}\right) S_v}{Y_3} \end{aligned}\right\}$$

Proved.**Numerical simulation**

This section offers numerical simulations designed to elucidate the dynamic characteristics of the Caputo fractional-order deterministic nonlinear mathematical model concerning Zika Virus. Utilizing MATLAB software and parameter values outlined in Tables 1, the simulations were executed. We choose the initial population to be Sp(0) = 300, Ep(0) = 0, Iap(0)=1, Isp(0)=1, Tsp(0) = 0, Rp(0) = 0, Sv(0) = 300, Ev(0) = 0, Iv(0) = 1.

Figures 2 through 9 present dynamic models for individual compartments, showcasing fractional variations, while Figures 10 through 15 demonstrate the influence of optimal control measures on human compartments. Additionally, Figures 16 through 18 showcase the effect of optimal control on vector compartments.

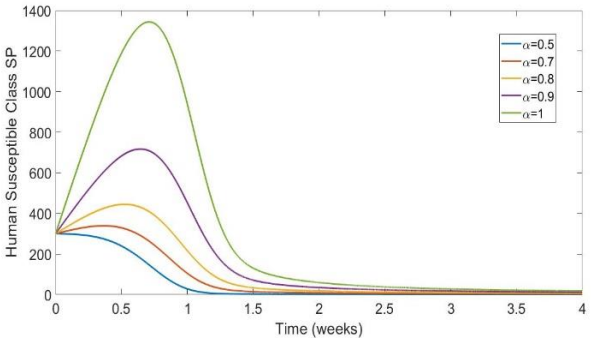

Figure 2: Simulation of Human Susceptible Class with fractional variations

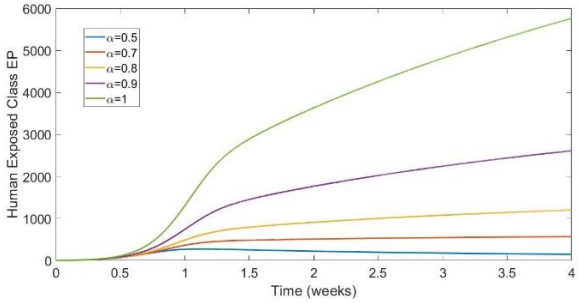

Figure 3: Simulation of Human Exposed Class with fractional variations

Cite this article as:
Loyinmi, A. C. (2024). A fractional-order model for zika virus transmission dynamics: analysis, control strategies, and simulation insights, *FNAS Journal of Scientific Innovations*, *6*(1), 84-108.

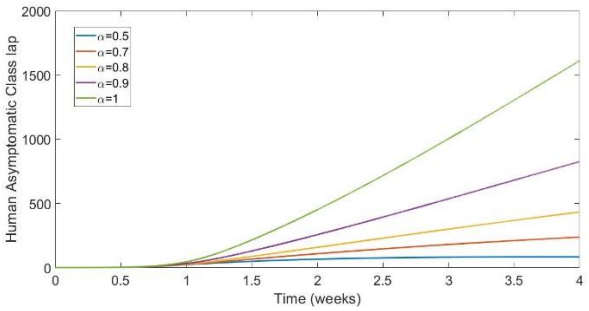

Figure 4: Simulation of Human Asymptomatic Class with fractional variations

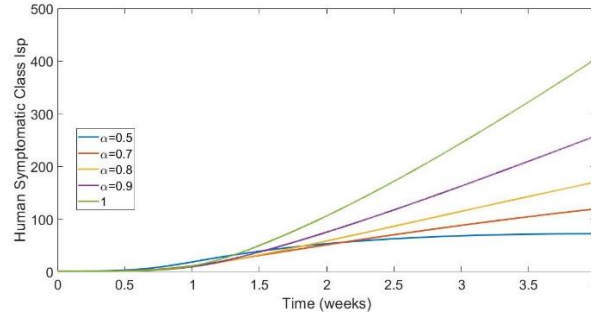

Figure 5: Simulation of Human Symptomatic Class with fractional variations

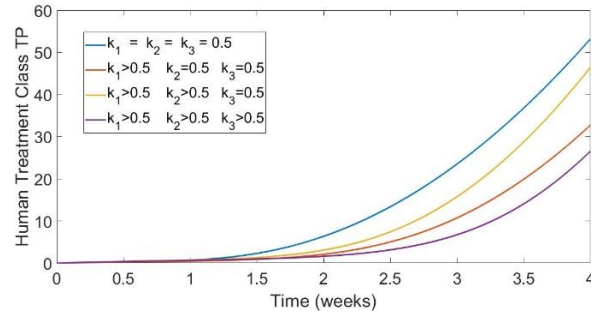

Figure 6: Simulation of Human Treatment Class with fractional variations

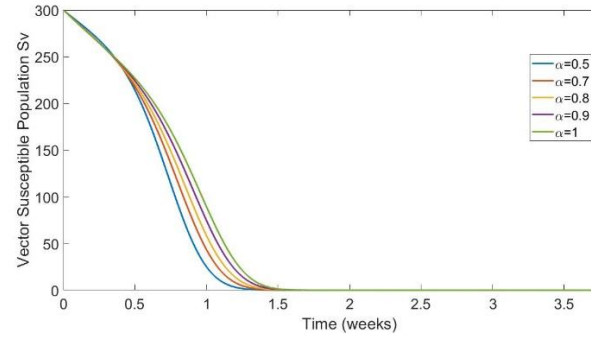

Figure 7: Simulation of Vector Susceptible Population with fractional variations

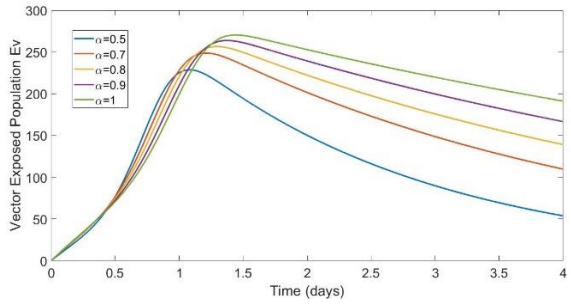

Figure 8: Simulation of Vector Exposed Population with fractional variations

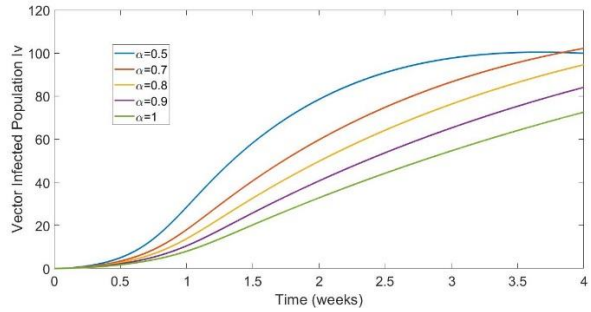

Figure 9: Simulation of Vector Infected Population with fractional variations

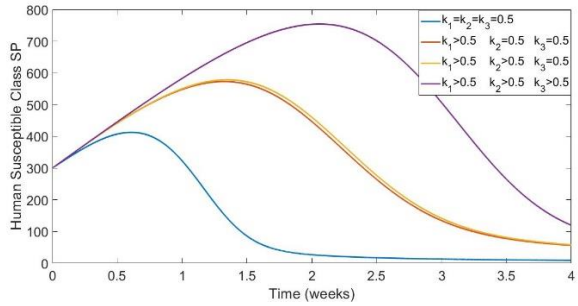

Figure 10: The optimal control on human susceptible population

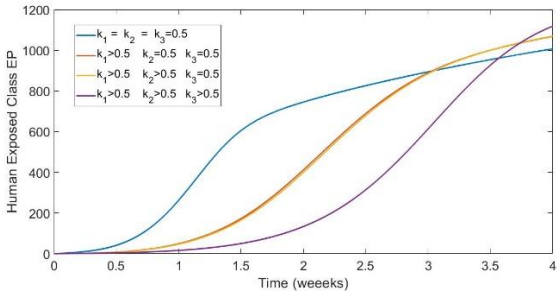

Figure 11:The optimal control on human exposed population

Cite this article as:
Loyinmi, A. C. (2024). A fractional-order model for zika virus transmission dynamics: analysis, control strategies, and simulation insights, *FNAS Journal of Scientific Innovations*, *6*(1), 84-108.

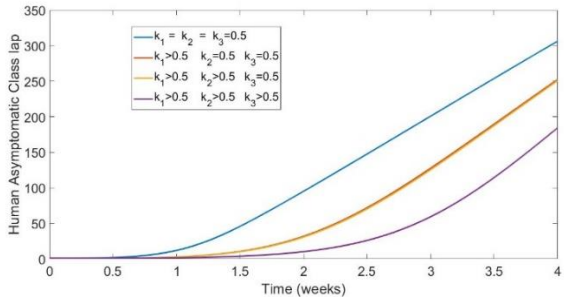

Figure 12: The optimal control on human asymptomatic population

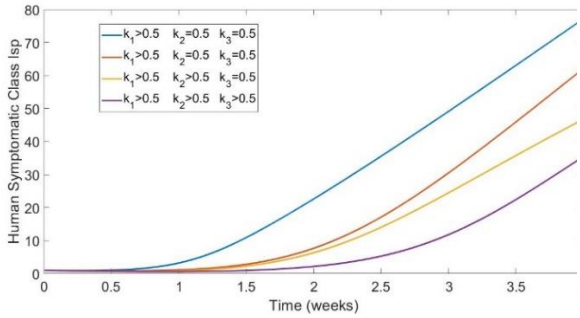

Figure 13: The optimal control on human symptomatic population

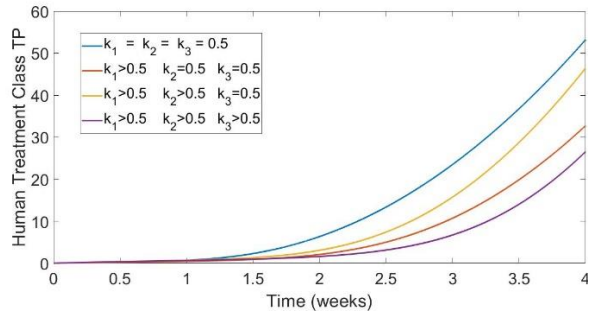

Figure 14: The optimal control on human treatment class

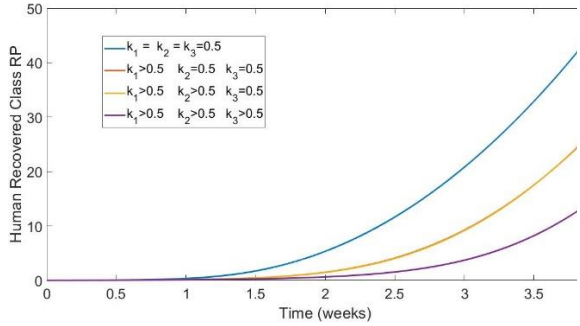

Figure 15: The optimal control on human recovered class

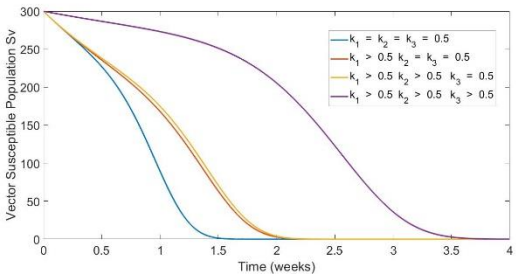

Figure 16: The optimal control on vector susceptible population

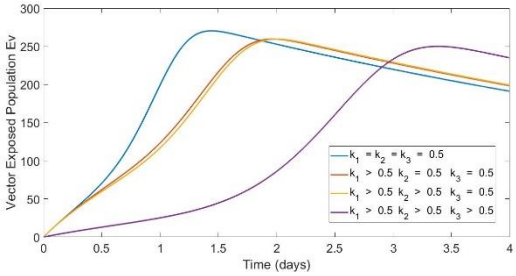

Figure 17: The optimal control on vector exposed population

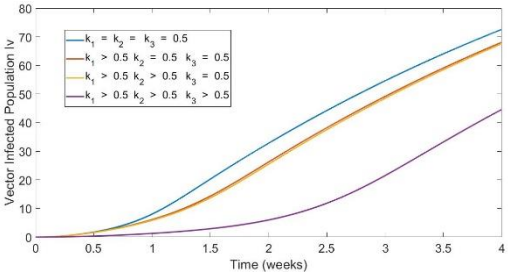

Figure 18: The optimal control on vector infected population

Discussion

Figures 2 through 9 provide a comprehensive visual representation of the dynamic intricacies inherent in Fractional Ordinary Derivative Equations (FODEs), showcasing their heightened efficacy as descriptors for biological systems

Cite this article as:
Loyinmi, A. C. (2024). A fractional-order model for zika virus transmission dynamics: analysis, control strategies, and simulation insights, *FNAS Journal of Scientific Innovations*, *6*(1), 84-108.

when compared to conventional integer-order models. Significantly, the depicted solutions of the model, governed by the continuous evolution of the time-fractional derivative, consistently demonstrate convergence towards equilibrium points.

Figure 10 illustrates the impact of optimal control measures on the human susceptible population in the context of Zika virus transmission. The graph shows that as the optimal control measures increase—specifically, through individual vaccination, treatment of symptomatic individuals, and environmental management—the number of susceptible individuals in the human population also increases. This trend indicates that effective control strategies successfully reduce the transmission rates, thereby preventing more people from becoming infected. Consequently, a higher proportion of the population remains susceptible but uninfected, highlighting the effectiveness of these combined interventions in managing the spread of the virus. Figure 11 illustrates the effect of optimal control on the human exposed population. Initially, as the optimal control measures are increased, there is a rise in the exposed human population for approximately three weeks. This initial increase can be attributed to the lag in the impact of control measures such as vaccination and treatment. However, beyond this period, the exposed population begins to decline as the effectiveness of these interventions becomes more pronounced. The subsequent reduction in the exposed population underscores the importance of sustained and intensified control efforts over time to mitigate the spread of the Zika virus. Figure 12 illustrates the impact of optimal control measures on the human asymptomatic population in the context of Zika virus transmission. As the level of optimal control increases, the size of the asymptomatic human population decreases significantly. This trend suggests that effective implementation of control strategies such as vaccination and treatment efforts can substantially reduce the spread of the virus by lowering the number of asymptomatic carriers who might unknowingly contribute to transmission. The figure underscores the importance of robust public health interventions in managing and mitigating the impact of Zika virus outbreaks. Figure 13 demonstrates the impact of optimal control strategies on the human symptomatic population of Zika Virus. As the optimal control, represented by the combined efforts of individual vaccination, treatment of symptomatic individuals, and environmental management, increases, the number of symptomatic individuals decreases. This indicates that higher levels of control measures effectively reduce the spread and impact of the Zika virus among humans. Specifically, the treatment of symptomatic individuals plays a crucial role in reducing the number of symptomatic cases, highlighting the importance of robust healthcare responses alongside preventive measures. Figure 14 depicts the relationship between the optimal control of human and the size of the treated human population. As the optimal control increases, indicating a higher effort in treating symptomatic individuals, it's observed that the treated human population decreases. This seemingly counterintuitive trend could suggest that the treatment efforts are effective in reducing the number of symptomatic cases over time, hence reducing the pool of individuals needing treatment. It underscores the potential effectiveness of intervention strategies in controlling the spread and impact of Zika virus through targeted human treatment. Figure 15 illustrates the impact of optimal control measures on the human recovered population in the context of Zika virus transmission dynamics. As the optimal control increases, indicating intensified efforts such as vaccination and treatment, the graph shows a decrease in the number of recovered individuals. This trend shows that while the control measures effectively reduce transmission and thus the number of infected individuals, they also influence the recovery rate, possibly due to altered disease dynamics or treatment efficacy. This emphasizes the complex interplay between intervention strategies and population-level outcomes in combating infectious diseases like Zika.

In Figure 16, the optimal control on the susceptible vector population is depicted. As the control increases, indicating higher efforts in environmental management like source reduction and water management, the susceptible vector population also increases. This counterintuitive relationship suggests that intensified environmental management might inadvertently create more breeding grounds for mosquitoes, leading to a rise in the susceptible vector population. This underscores the complexity of disease control strategies, emphasizing the need for comprehensive understanding and careful calibration of interventions to achieve desired outcomes effectively in combating Zika virus transmission. Figure 17 depicts the impact of optimal control measures on the exposed vector population over time. As the control effort increases, initially, there's a notable decrease in the exposed vector population, suggesting effective management strategies such as environmental interventions. However, after approximately two weeks, the exposed vector population begins to rise again. This implies a potential resurgence of vector populations due to factors like environmental changes or diminishing effectiveness of control measures over time. Further analysis would be needed to understand the dynamics driving this observed trend and to optimize control strategies accordingly. Figure 18 depicts the impact of optimal control measures on the infected vector population in the context of Zika virus transmission. As the level of optimal control increases, indicating intensified

Cite this article as:
Loyinmi, A. C. (2024). A fractional-order model for zika virus transmission dynamics: analysis, control strategies, and simulation insights, *FNAS Journal of Scientific Innovations*, *6*(1), 84-108.

efforts such as environmental management, the infected vector population diminishes. This reduction suggests a successful intervention in curbing Zika virus transmission within the vector population, possibly through strategies like source reduction, water management, and urban planning. The figure underscores the effectiveness of proactive measures in mitigating the spread of Zika by targeting the vector population, essential for controlling disease transmission dynamics.

Conclusion

The optimal control measures implemented for managing Zika virus transmission exhibit promising outcomes across both human and vector populations. As depicted in Figures 10-15, interventions such as vaccination, treatment, and environmental management effectively reduce transmission rates among humans, leading to fewer symptomatic cases and a lower overall impact of the virus. However, the complexities of disease dynamics are evident, as seen in Figures 16-18, where intensified environmental management initially increases the susceptible vector population but ultimately diminishes the infected vector population. This underscores the importance of comprehensive understanding and ongoing assessment of control strategies to effectively combat Zika virus transmission dynamics.

Recommendations

Mathematical framework of the current study on Zika virus can be extended to include parameter estimation and sensitivity analysis.

References

Agbomola, J.O., & Loyinmi, A.C. (2022). Modelling the impact of some control strategies on the transmission dynamics of Ebola virus in human-bat population: An optimal control analysis. *Heliyon*, 8:e12121. https://doi.org/10.1016/j.heliyon.2022.e12121.

Agusto, F.B., Bewick, S., & Fagan, W.F. (2017). Mathematical model for Zika virus dynamics with sexual transmission route. *Ecol Complex*. 29, 61–81. doi: 10.1016/j.ecocom.2016.12.007

Alfwzan, W.F., Raza, A., Martin-Vaquero, J., Baleanu, D., Rafiq, M., & Ahmed, N. (2023). Modeling and transmission dynamics of Zika virus through efficient numerical method. *AIP Advan*., 13, 095221. doi: 10.1063/5.0168945.

Andraud, M., Hens, N., Marais, C., & Beutels, P. (2012). Dynamic epidemiological models for dengue transmission: A systematic review of structural approaches. *PloS one*, 7, e49085

Banuelos, S., Martinez M., Mitchell C., & Prieto-Langarica. (2019). Using mathematical modelling to investigate the effect of the sexual behaviour of asymptomatic individuals and vector contrl measures on Zika. *Letters in Biomathematics*, 6(1), 1-19.

Bearcroft, W.G.C. (1956). Zika virus infection experimentally induced in a human volunteer. *Transactions of the Royal Society of Tropical Medicine and Hygiene*, 50, 442–448.

De Araújo, T.V.B., Ximenes, R.A., de A., Miranda-Filho D., & De. B. (2022). Association between microcephaly, Zika virus infection, and other risk factors in Brazil: Final report of a case-control study. *Lancet Infect Dis*. 3099(17), 30727-82

Duffy, M. R.., Chen, T.H., Hancock, W. T., Powers, A. M., Kool, J. L., Lanciotti, R. S., & Hayes, E. B. (2009). Zika virus outbreak onyap island, federated states of micronesia. *New England Journal of Medicine*, 360(24), 2536–2543.

Gonzlez-Parra. G., Daz-Rodrguez., M., & Arenas, A.J. (2020). Optimization of the controls against the spread of Zika virus in populations. *Computation*, 8(76). doi: 10.3390/computation8030076

Griffin, M. P. (2012). Modeling the effects of malaria preventative measures, *SIAM Undergraduate Research Online* (SIURO), 6. doi:10.1137/12S011805

Hayes, E.B. (2009). Zika virus outside Africa, *Emerg. Infect. Dis*., 15, 1347–1350. doi:10.3201/eid1509.090442.

Idowu, O. K., & Loyinmi, A.C. (2023). Qualitative analysis of the transmission dynamics and optimal control of covid-19. *EDUCATUM Journal of Science, Mathematics and Technology*, 10: 1, 54-70. https://doi.org/10.37134/ejsmt.vol10.1.7.2023.

Khan, M. A., & Atangana, A. (2020). Modeling the dynamics of novel coronavirus (2019-nCoV) with fractional derivative. *Alexandria Eng J*., 599, 2379–89. doi: 10.1016/j.aej.2020.02.033

Khan, M. A., Wasim, Shah, A., Ullah, S., & Gmez-Aguilar, J.F. (2019). A dynamical model of asymptomatic carrier Zika virus with optimal control strategies. *Nonlinear Anal Real World Appl*., 50:144–70. doi: 10.1016/j.nonrwa.2019.04.006.

Kibona, I. E., & Yang, C.H. (2017). SIR model of spread of Zika virus infections: Zikv linked to microcephaly simulations, *Health*, 9, 1190–1210. doi: 10.4236/health.2017.98086

Krauer. F., Riesen. M., & Reveiz. L. (2017). Zika virus infection as a cause of congenital brain abnormalities and guillain–barré syndrome: Systematic review. *PLoS Med*., 14(1), doi:10.1371/journal.pmed.10022

Loyinmi, A.C, Akinfe, T.K., & Ojo, A. A. (2021). Qualitative analysis and dynamical behavior of a Lassa haemorrhagic fever model with exposed rodents and saturated incidence rate. *Sci. African*, 14; e01028. https://doi.org/10.1016/j.sciaf.2021.e01028.

Loyinmi, A.C., Gbodogbe, S.O., & Idowu, K.O. (2023). On the interaction of the human immune system with foreign body: mathematical modeling approach. *Kathmandu University Journal of Science, Engineering and Technology*, 17(2), 1-17. https://journals.ku.edu.np/kuset/article/view/137

Loyinmi, A. C., Ajala, A. S., & Alani, L. I. (2024). Analysis of the effect of vaccination, efficient surveillance and treatment on the transmission dynamics of cholera. Al-Bahir journal for Engineering and Pure Sciences, 5(2), 94 – 107. https://doi.org/10.55810/2313-0083.1070

Loyinmi, A.C., & Gbodogbe, S.O. (2024). Mathematical modeling and control strategies for Nipah virus transmission incorporating Bat – to – pig –to – human pathway. *EDUCATUM Journal of Science, Mathematics and Technology*, 11(1), 54-80. https://doi.org/10.37134/ejsmt.vol11.1.7.2024

Loyinmi, A.C., & Ijaola, A.L. (2024). Fractional order model of dynamical behavior and qualitative analysis of Anthrax with infected vector and saturation. *Preprints*, 2024030632. https://doi.org/10.20944/preprints202403.0632.v1

Mehrjardi, M. Z. (2017). Is Zika virus an Emerging TORCH agent? An invited commentary, Virology, *Res. Treat*., 8, 1–3. doi: 10.1177/1178122X17708993

Musso. D., Ko, A.I., & Baud, D. (2019). Zika Virus Infection – After the Pandemic. *N Engl J Med*., 381(15). doi:10.1056/nejmra1808246

Padmanabhan, P., Seshaiyer, P., & Castillo-Chavez, C. (2017). Mathematical modeling, analysis and simulation of the spread of Zika with influence of sexual transmission and preventive measures. *Letters in Biomathematics*, 4(1), 148-166

Rezapour. S., Mohammadi, H., & Jajarmi A. (2020). A new mathematical model for Zika virus transmission. *Adv Diff Equ*.,:1–15. doi: 10.1186/s13662-020-03044-7

Sikka, V., Chattu, V.K., Popli, R.K., Galwankar, S.C., Kelkar, D., & Sawicki, S.G. (2016). The emergence of Zika virus as a global health security threat: A review and a consensus statement of the INDUSEM Joint Working Group (JWG), *J. Glob. Infect. Dis*., 8, 3–15. doi: 10.4103/0974-777X.176140

Tesla, B., Demakovsky, L.R., Mordecai, E.A., Ryan, S.J., Bonds, M.H., & Ngonghala, C.N. (2018). Temperature drives Zika virus transmission: evidence from empirical and mathematical models. *Proc R Soc B*., 285,. doi: 10.1098/rspb.2018.0795

Yun, S.I., & Lee, Y.M. Zika virus. (2017). An emerging flavivirus. *J Microbiol*., 55, 204–19. doi: 10.1007/s12275-017-7063-6